

Cover page

Title: Toxin resistance mechanisms span biological scales in the Royal Ground Snake (Colubridae: *Erythrolamprus reginae*)

Authorships: Ramírez-Castañeda V.^{1*}, Nixon S. A.², Alarcón-Naforo D.³, Abderemane-Ali F.⁴, Fitch R. W.⁵, Salazar-Valenzuela D.⁶, Minor, Jr. D. L.^{2,7,8,9,10}, Tarvin R. D.¹

Affiliations:

¹Museum of Vertebrate Zoology and Department of Integrative Biology, University of California, Berkeley, CA, 94720, USA

²Cardiovascular Research Institute, University of California, San Francisco, CA, 94158

³Departamento de Biología, Facultad de Ciencias, Universidad Nacional de Colombia, Bogotá, Colombia

⁴Department of Physiology, David Geffen School of Medicine, University of California, Los Angeles, CA, 90095, USA

⁵Department of Chemistry and Physics, Indiana State University, Terre Haute, IN, 47809, USA

⁶Centro de Investigación de la Biodiversidad y Cambio Climático (BioCamb) e Ingeniería en Biodiversidad y Recursos Genéticos, Facultad de Ciencias de Medio Ambiente, Universidad Indoamérica, Av. Machala y Sabanilla, Quito, Ecuador

⁷Departments of Biochemistry & Biophysics, and Cellular & Molecular Biology, University of California, San Francisco

⁸California Institute for Quantitative Biomedical Research, University of California, San Francisco

⁹Kavli Institute for Fundamental Neuroscience, University of California, San Francisco

¹⁰Molecular Biophysics and Integrated Bio-imaging Division, Lawrence Berkeley National Laboratory, Berkeley, CA

*vramirez@berkeley.edu

Abstract:

Exposure to multiple toxic compounds imposes diverse selective pressures, potentially leading to a toxin-resistant phenotype that operates across biological levels. There are several known toxin resistance mechanisms—such as behavioral avoidance, metabolic detoxification, and target-site insensitivity. However, most studies have been conducted with exposure to a single toxin or have focused on only one of these mechanisms. More integrative approaches are necessary to capture the complexity of the toxin-resistant phenotype in a single organism. Predators of amphibians, for example, must counteract multiple chemicals secreted by different species or even by the same individual prey. The pan-Amazonian snake *Erythrolamprus reginae* (Squamata: Colubridae) preys on multiple species of poisonous frogs, including members of the Dendrobatidae family, and is therefore exposed to a chemically diverse diet. We aimed to evaluate the process of consuming a toxic prey, from behavioral decisions to a suite of possible resistance mechanisms. We tested interrelated hypotheses to understand the complexity of toxin resistance in *E. reginae*. First, feeding assays revealed that *E. reginae* exhibited longer handling times and aversive behaviors toward the highly toxic *Ameerega trivittata*, suggesting that prey toxicity imposes searching and handling costs that influence foraging strategies. Second, we developed a novel assay to screen liver extracts for toxin neutralization and showed that soluble proteins in the liver partially restored sodium channel activity inhibited by *A. trivittata*

alkaloids and neosaxitoxin, indicating the presence of toxin-binding proteins that mediate detoxification. Third, transcriptomic profiling across tissues revealed liver-specific upregulation of transporters, such as the solute carrier protein family, and stress-response genes following exposure to *A. trivittata*, supporting a complementary detoxification mechanism. Finally, using two-electrode voltage-clamp recordings, we showed that one variant of the *E. reginae* muscle-expressed voltage-gated sodium channel $\text{Na}_v1.4$ is highly resistant to tetrodotoxin, saxitoxin, and neosaxitoxin. However this same $\text{Na}_v1.4$ channel variant did not prevent inhibition by *A. trivittata* alkaloids, suggesting that resistance to these compounds relies on alternative mechanisms such as the putative liver binding proteins. These findings demonstrate that *E. reginae* populations may be adapting to a chemically diverse diet by evolving multiple, overlapping forms of resistance, highlighting the complexity of resistance where selection favors multiple mechanisms acting at different physiological levels to mitigate the effects of prey toxins. This study provides unparalleled insight into whole-organismal resistance to toxin ingestion, advancing our understanding of the genetic architecture underlying toxin adaptation and its broader physiological and evolutionary implications.

Key words: Toxin resistance, *Erythrolamprus reginae*, predation, toxin-binding proteins, solute carrier proteins, target-site resistance

Introduction

Small molecule toxins often exert strong effects in ecological interactions, mostly by serving as chemical defenses against predation or herbivory (Ferrer and Zimmer 2012; Ferrer and Zimmer 2013). Both predators and prey require molecular strategies to cope with these compounds in their environments. Exposure to multiple toxic compounds imposes diverse selective pressures, potentially leading to a toxin-resistant phenotype that operates across biological levels (Tarvin et al. 2023). Predators of amphibians, for example, have to counteract multiple chemicals secreted from different species or even from the same individual prey (Daly 1995; Daly 1998; Saporito et al. 2011). As a result, predators evolve various mechanisms to avoid or limit exposure to the toxins they encounter. However, some predators do not avoid toxin exposure and have thus evolved to resist toxins through multiple behavioral, physiological, and molecular adaptations. The specifics of these adaptations depend not only on the organism that evolved them but also on the effect and level of exposure to the particular toxins involved (Tarvin et al. 2023). Understanding such traits requires an integrative approach because of the inherent system complexity.

The pan-Amazonian Royal Ground snake *Erythrolamprus reginae* (Squamata: Colubridae) is exposed to a variety of toxins through its diet. Observations report that these snakes are generalist predators that consume multiple species of poisonous frogs, including members of the Bufonidae and Dendrobatidae families (Albarelli and Santos-Costa 2010; Pašukonis and Loretto 2020). Notably, it consumes the three-striped poison frog (*Ameerega trivittata*), which secretes multiple neurotoxic compounds (Daly 1995; Santos et al. 2016; Pašukonis and Loretto 2020). Recent studies indicate that *E. reginae* harbors mutations in voltage-gated sodium channels (Na_v) associated with resistance to tetrodotoxin (TTX) and saxitoxin (STX) (Ramírez-Castañeda et al., 2024). This suggests that toxin resistance in *E. reginae* involves adaptations to multiple toxins through mechanisms such as target-site resistance (TSR) in Na_v channels.

However, to develop a more comprehensive perspective that better reflects natural systems, it is necessary to evaluate multiple resistance mechanisms. Although TSR is a well-documented

mechanism, a predominant focus on it in the literature may underestimate other important resistance strategies, leading to a biased view of how toxin resistance evolves (Tarvin et al. 2023). For instance, resistance can also arise through the upregulation of enzymes with xenobiotic activity rapid excretion, the formation of diffusion barriers or via soluble proteins that sequester toxins, preventing their interaction with target sites (reviewed by Tarvin et al. 2023). Metabolic resistance may or may not be toxin-specific and represents a fundamental part of an organism's baseline detoxification processes. Any or all of these mechanisms may be active in any given toxin-resistant higher organism.

Another mechanism involves the production of proteins that mimic the toxin's target, binding and sequestering the toxin before it reaches its site of action. This strategy is usually toxin-specific and has been documented in frogs for saxitoxin (STX) via the high affinity STX-binding protein saxiphilin (Sxph) and for STX and tetrodotoxin (TTX) in pufferfish via the pufferfish saxitoxin and tetrodotoxin binding protein (PSTBP) (Mahar et al. 1991; Morabito and Moczydlowski 1995; Yotsu-Yamashita et al. 2001; Yen et al. 2019; Chen et al. 2022). Radiolabelled STX binding studies have also suggested the presence of STX-binding proteins in reptiles, amphibians, fish, and arthropods (Llewellyn et al. 1997; Tarvin et al. 2023).

Here we aim to unravel the complexity of toxin resistance in this snake species by tracing several biological scales where toxins may influence the evolution of resistant traits, from behavioral decisions to consume toxic prey, to the suite of possible molecular resistance mechanisms. We employ multiple methods to investigate this paradigm by: 1) Observing predation behavior to assess interactions with toxic prey; 2) investigating the expression of detoxifying proteins in several organs, and 3) evaluating the resistance conferred by target-site resistant (TSR) mutations against different toxins present in the snake's diet.

Our findings show that, in the presence of multiple toxic prey, diverse toxin-resistant phenotypes emerge to cope with the ingestion of small bioactive molecules. These adaptations may shape ecological interactions and evolutionary dynamics within the community, while also contributing to our understanding of physiological responses to toxin exposure, insights that may have relevance beyond ecological systems, including biomedical research.

Results and Discussion

***E. reginae* snakes exhibit avoidance and specific behaviors when feeding on toxic poison frog prey (*Ameerega trivittata*)**

In the process of predation, a predator must first encounter a prey item and then decide whether or not to consume it. *E. reginae* is a predator that encounters and consumes several types of toxic prey species. While toxic prey are traditionally considered a low-quality food source due to the energetic trade-offs between prey nutrition and the harmful effects of their toxins (Marshall 1908; Speed 1993; Sherratt 2003; Sherratt et al. 2004; Skelhorn et al. 2011; Halpin et al. 2013; Mappes et al. 2014; Rowland et al. 2017), and many studies assume that predators avoid toxic prey, some—such as *E. reginae*—clearly do not. One reason for this discrepancy is that the trade-off between nutrition and toxicity may be minimized for resistant predators. Most toxic prey studies, outside herbivory research, focus on aposematism in lab-trained predators or are conducted using prey models (Darst and Cummings 2006; María Arenas et al. 2015; Halpin et al. 2020), yet little is known about predator behavior in natural settings. Here, we tested whether

behavioral avoidance or tolerance can be observed in a toxin-resistant predator when it encounters a sympatric toxic prey, compared to a non-toxic prey. Bridging this gap can help connect theoretical and experimental approaches with real-world ecological interactions.

We offered adult *E. reginae* snakes from Leticia, Amazonas, Colombia (Table S1) (fasted for five days) a set of locally co-occurring frog prey with diverse chemical defenses and toxicity levels. The only highly toxic frog included was the dendrobatid *Ameerega trivittata*, which secretes histrionicotoxins (HTX), pumiliotoxins (PTX), and decahydroquinolines (DHQ) (Daly 1995; Santos et al. 2016). The other frogs included species of hylids reported to be non-toxic, primarily *Scinax ruber*, as well as *Dendropsophus* sp. and *Sphaenorhynchus lacteus*. Additionally, some snakes were offered mildly toxic frogs, *Leptodactylus* sp. and *Rhinella margaritifera*, which secrete amines and steroidal toxins (respectively) (Ceï et al. 1967; Daly et al. 1987; Prates et al. 2012). However, many snakes are not sensitive to the effects of the steroidal toxins (e.g., bufadienolides) because of TSR mutations in their sodium-potassium pumps (Ujvari et al. 2015; Mohammadi et al. 2016). Chemical analysis using gas chromatography mass spectrometry (GC/MS) confirmed the presence of multiple neurotoxic alkaloids from *A. trivittata* whole skin ($n = 6$), including DHQs, N-methyl-DHQs, 5,8-indolizidines, and HTXs, consistent with prior literature (Daly 2005). No alkaloids were detected from *S. ruber* whole skin ($n = 6$); other species were not tested (Dataset S6). Interestingly, when offered *A. trivittata*, only 4 of 10 snakes were willing to consume this prey, and one of these individuals died after ingestion (Fig. 1A-B, Dataset S1-S2). If the snake did not consume *A. trivittata* within two hours, we then removed the *A. trivittata* from the cage and offered the snake another prey option (e.g., *S. ruber*, *Dendropsophus* sp., *Sphaenorhynchus lacteus*, *Leptodactylus* sp., or *R. margaritifera*). All 6 of the snakes that refused to consume *A. trivittata* consumed the second prey that was offered, usually within one minute. Snakes also showed significant differences in the handling and consumption of *A. trivittata* versus other prey by taking longer to swallow them (Fig. 1C) and exhibiting a unique "dragging" behavior—rubbing the frog along the ground (see video Dataset S2 and YouTube (<https://youtube.com/shorts/CUsNjgG3jTA?feature=share>)). This behavior was exclusively observed during ingestion of *A. trivittata*, and not with any other frog prey (Fig. 1D). Rubbing the frog on the ground may help remove or break down some of the toxins, a hypothesis that requires further testing. Similar toxin-avoidance behaviors such as dragging, wiping, or washing prey, have been reported in several bird predators. For example, the hooded merganser (*Lophodytes cucullatus*), the southern ground hornbill (*Bucorvus leadbeateri*), and the grey heron (*Ardea cinerea*) exhibit these behaviors when feeding on frogs and toxic newts (Kemp and Kemp 1978; Underhill 2015; Smith et al. 2024). This suggests that there is increased time and/or energy expended when handling highly toxic prey (Hurlbert 1970). Our findings demonstrate a clear preference for prey other than the toxic *A. trivittata* by *E. reginae* and underscore challenges posed by toxic prey at the organismal level, as reflected in distinct behavioral responses and survival outcomes.

Optimal foraging theory predicts that predators may consume toxic prey when the alternative is less nutritious (Halpin et al. 2013; Halpin et al. 2014) or more difficult to locate (Carle and Rowe 2014). However, multiple factors seem to influence this type of foraging behavior, such as the predator physiological state; starved predators increase toxic prey consumption when alternatives are scarce (Aubier and Sherratt 2020), and those in high-energy states make decisions based on prior experiences with toxic prey (Skelhorn and Rowe 2007). Further ecological and behavioral analyses are necessary to determine the physiological and/or ecological factors that motivate *E. reginae* to feed on *A. trivittata*, a less preferred prey that is more energetically challenging to consume. However, as shown, *E. reginae* likely regularly include a gradient of palatable/non-palatable prey in their diet (e.g: *R. margaritifera* and *Leptodactylus* sp.), probably resulting from the context and community specific foraging

decisions (Skelhorn et al., 2016) and presence of additional toxin resistance mechanisms. Therefore, unprofitability/profitability is not a binary variable but instead a gradient of factors that depend on the physiology, prey community, toxin resistance efficiency, and experience of the predator.

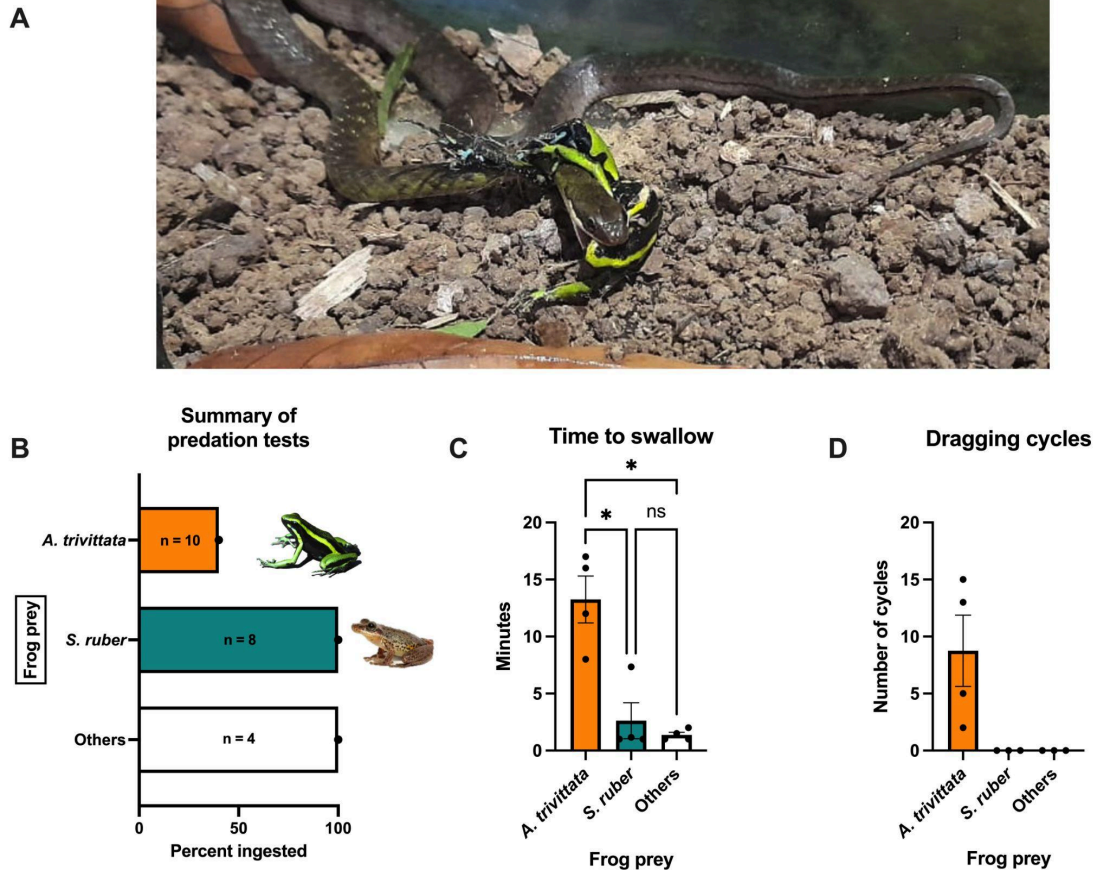


Figure 1. *E. reginae* presented longer swallowing times and a dragging behavior when feeding on the poisonous frog *A. trivittata*. (A) *Erythrolamprus reginae* feeding on a three-striped poison frog (*Ameerega trivittata*), photographed by Leonardo Castañeda. (B) Summary of predation trials and ingestion percentages. *A. trivittata* (high alkaloid content) was offered to *E. reginae* 10 times, of which only four frogs were consumed. One snake died after *A. trivittata* ingestion. *S. ruber* (no alkaloids) was offered eight times, and all were consumed, as well as four individuals of other frog species (1 *Dendropsophus* sp., 1 *Leptodactylus* sp., 1 *Rhinella margaritifera* and 1 *Sphaenorhynchus lacteus*) that were offered. (C) Comparison of swallowing time between *E. reginae* feeding on *A. trivittata*, *S. ruber*, and other species revealed a significant difference (Kruskal-Wallis test; (*) $P \leq 0.05$). (D) Analysis of drag cycle behavior during predation revealed that this behavior was exhibited only when feeding on *A. trivittata*. In contrast, no such behavior was observed when feeding on *S. ruber* or other species.

Soluble liver proteins contribute to *E. reginae* ability to consume *A. trivittata*

Once swallowing occurs and toxin ingestion is not avoided, predators rely on resistance mechanisms that involve either metabolizing the toxin and/or modifying its target (Tarvin et al.

2023). In vertebrates, the liver is the primary organ responsible for blood detoxification via enzymatic oxidation and conjugation. Proteins that reduce the toxicity of a compound include detoxifying enzymes that modify or degrade toxins, and/or soluble proteins that bind to toxins thereby preventing their interaction with target, such as the high-affinity STX binding protein Sxph found in diverse Anurans (Morabito and Moczydlowski 1995; Yen et al. 2019; Chen et al. 2022). We therefore investigated whether soluble proteins are contributing to the *E. reginae* toxin resistance phenotype.

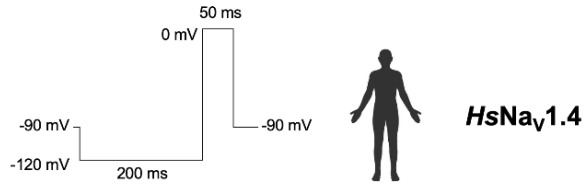
We focused on toxins relevant to *E. reginae*'s diet with activity on Na_v channels, particularly the potent Na_v blockers TTX, STX and neosaxitoxin (neoSTX) that *E. reginae* has been predicted to be resistant against from previous TSR studies (Ramírez-Castañeda et al., 2024). We first established the activity of these toxins against mammalian cells stably expressing the human skeletal muscle Na_v isoform (*HsNa_v1.4*) using semi-automated planar patch-clamp electrophysiology, and found half-maximal inhibitory (IC₅₀) values in line with previous studies (0.35 ± 0.06 nM, 4.3 ± 0.35 nM and 17.2 ± 6.8 nM for neoSTX, STX and TTX respectively, Supplementary Fig. S2) (Alonso et al. 2016; Zakrzewska et al. 2025). We then selected concentrations sufficient to block approximately 90% of the *HsNa_v1.4* current (neoSTX: 1.5 nM, STX: 100 nM, TTX: 300 nM). We also tested *A. trivittata* skin secretion (diluted 1:200) and naturally occurring poison frog alkaloids: pumiliotoxin 251D (PTX251D); H₈-histrionicotoxin (H₈-HTX); and histrionicotoxin-283A (HTX283A), isolated from mixed frog collections (Daly, 2005; Santos et al., 2016). Due to scarce material and the lower affinity against *HsNa_v1.4*, these toxins were tested at single concentrations sufficient to block *HsNa_v1.4* by at least 60%: PTX251D, 500 μM; H₈-HTX, 250 μM; HTX283A, 500 μM.

We then developed a novel assay for screening liver extracts for functional toxin neutralization. We first pre-treated *A. trivittata* skin extract or toxins with *E. reginae* liver extract (0.2 mg/mL final concentration) for 30 minutes at room temperature, to allow possible toxin resistance proteins to sequester or modify the toxins. We then used semi-automated planar patch-clamp electrophysiology to compare *HsNa_v1.4* currents sequentially elicited under saline (baseline), toxin/skin extract alone, liver extract-treated toxin, and liver extract alone (see schematic in Supplementary Fig. S3). Restoration of channel activity in the presence of the preincubated toxin:liver extract, relative to baseline and toxin-alone block, was interpreted as evidence for detoxifying or toxin-binding proteins in the liver (Fig. 2). *E. reginae* liver extracts were compared against liver extracts from two control (toxin-sensitive) species: the house mouse (*Mus musculus*) and another colubrid snake, *Contia tenuis*. All tested liver extracts were confirmed to not significantly inhibit *HsNa_v1.4* currents when applied by themselves (Fig. 2B, Supplementary Fig. S4 and S5). Remarkably, preincubation of *E. reginae* liver extract inhibited toxin block by all poison frog alkaloids tested, with the greatest current recovery observed for HTX283A (mean 76.3 ± 9.1%, Fig. 2B). This effect also extended to modest recovery from *A. trivittata* skin extract block (16.6 ± 2.7%, Fig. 2A) and moderate recovery of neoSTX (61.1 ± 6.0%, Fig. 2F). By contrast, control mouse liver extract did not restore sodium channel activity for any toxin condition (Fig. 2 and Supplementary Fig. S4), indicating that amelioration of the toxin block was not driven by general vertebrate liver detoxification enzymes. *C. tenuis*, a Californian snake with no known natural exposure to *A. trivittata* or other dendrobatid toxins—and therefore no selection pressure for resistance—was used as an ecological control. *C. tenuis* liver extract had no effect on any dendrobatid toxin, STX, or TTX sodium channel block, but completely ameliorated neoSTX block (mean current recovery 91.5 ± 7.4%) (Fig. 2F and Supplementary Fig. S5). These findings suggest that detoxifying proteins in the *E. reginae* liver are ecologically specific, targeting toxins present in *A. trivittata* secretions and potentially enabling *E. reginae* to tolerate a toxic prey niche. Interestingly, none of the liver extracts affected *HsNa_v1.4* block by STX or TTX,

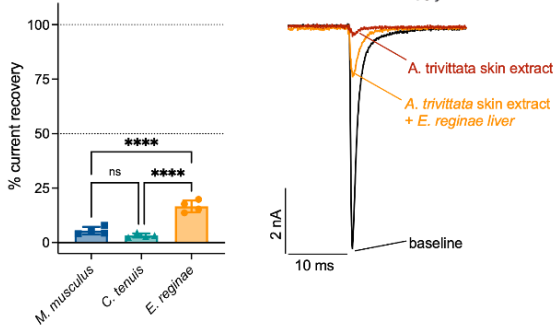
suggesting that *E. reginae* may rely on alternative resistance strategies to avoid poisoning by these potent neurotoxins.

Although *E. reginae* liver extract reduced the inhibitory effects of PTX251D, H₈-HTX, HTX283A, and *A. trivittata* skin secretion on HsNa_v1.4 activity, some toxin block remained (Fig. 2). This suggests that while the liver may reduce the impact of these toxins, there may still be some physiological cost associated with consuming *A. trivittata*, which may explain the snakes' reduced preference for this diet. Alternatively, the high concentrations of dendrobatid toxins used in the present study (250–500 μM) may have exceeded the neutralizing capacity of the liver extract. Due to limited toxin and liver material, we were unable to test varying ratios of toxin:liver extract to explore these potential thresholds. It would also be of interest to explore other higher affinity pharmacological targets of dendrobatid toxins, such as nicotinic acetylcholine receptors for HTX, where lower toxin requirements may be completely neutralized by the liver extract.

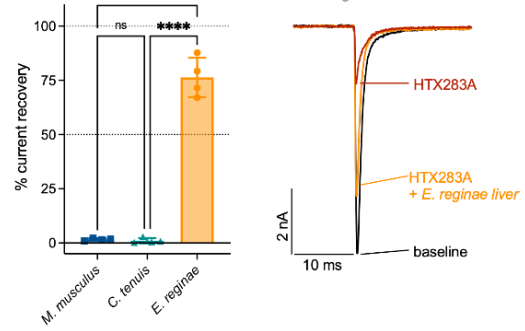
Intriguingly, while *E. reginae* liver extract had no effect on the very high-affinity Na_v toxins, TTX and STX, it restored the majority of HsNa_v1.4 current from the closely related structural analogue, neoSTX (Fig. 2F). These toxins were tested at much lower concentrations (1.5–300 nM) than the low-affinity dendrobatid toxins, which suggests that the detoxification mechanisms in *E. reginae* liver show remarkable chemical specificity between ecologically relevant toxins and even within alkaloid classes, rather than simply concentration-dependent toxin modulation. However, while total protein was standardized for these assays, the identity, relative abundance and affinities of the protein or soluble proteins contributing to detoxification within the total liver extracts are currently unknown. We further cannot exclude the possibility that the stability or functionality of potential toxin-binding proteins may have been impaired or even lost during the extraction process. Increasing the incubation time for the liver:toxin extracts may also further modulate the toxin effects. Further work is therefore needed to identify and characterize these proteins to understand their target affinities and selectivity and mechanisms of action. Additionally, gene expression related to detoxification may vary under different conditions, potentially increasing the liver's detoxifying capacity in response to toxin exposure. This is particularly relevant since the tissues used in this study were obtained from fasting snakes, rather than from individuals exposed to toxins. Nonetheless, it is remarkable that *E. reginae* liver protein extracts modulated the inhibitory effects of these toxins, even at the high concentrations needed for the dendrobatid toxins to block HsNa_v1.4 (250–500 μM, Fig. 2), underscoring liver detoxification as a key mechanism of toxin resistance for *E. reginae*.



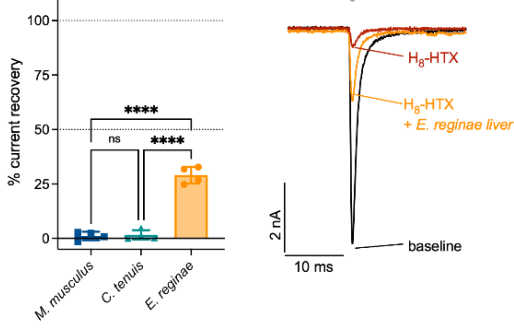
A *A. trivittata* skin extract



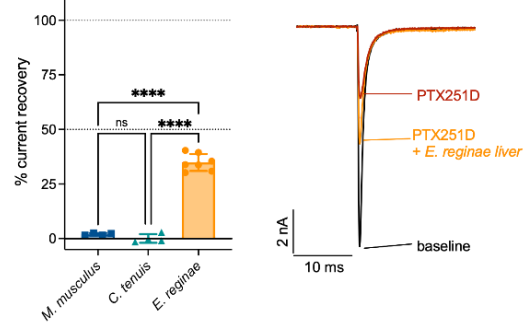
B HTX283A



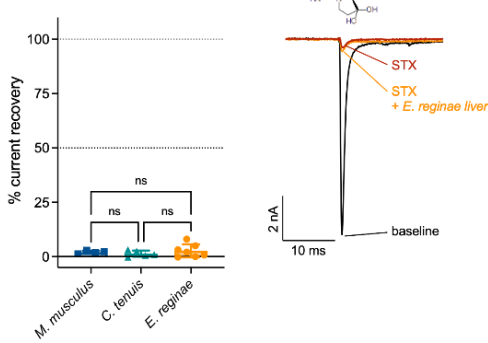
C H₈-HTX



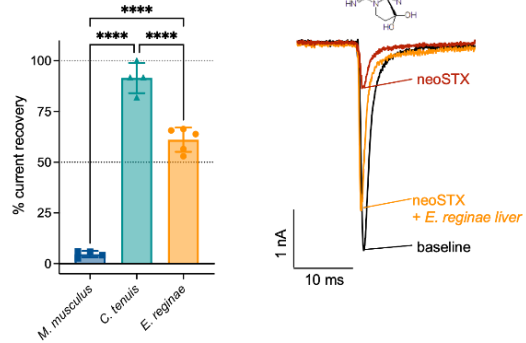
D PTX251D



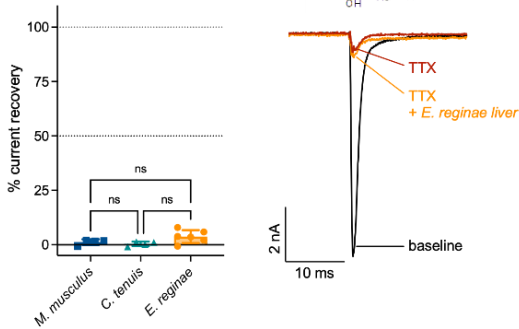
E STX



F neoSTX



G TTX



H Liver alone

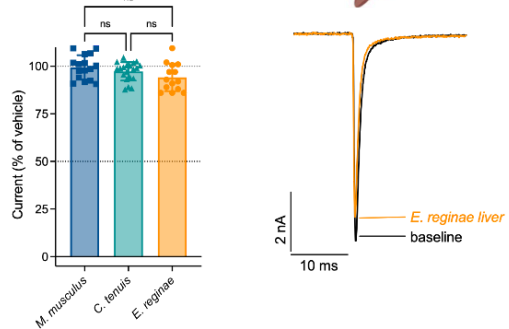


Figure 2. *E. reginae* liver extract mitigates dendrobatid toxin and neoSTX block of *HsNa_v1.4*, providing evidence of liver proteins involved in detoxification. Concentrations used: (A), *A. trivittata* skin extract, diluted 1:200; (B), HTX283A, 500 μ M; (C), H₈-HTX, 250 μ M; (D), PTX251D, 500 μ M; (E), STX, 100 nM; F, neoSTX, 1.5 nM; G, TTX, 300 nM; H, liver extract alone, 0.2 mg/mL. For all toxins and extracts, exemplar whole-cell patch-clamp recordings of *HsNa_v1.4* expressed in CHO cells are plotted in the absence of toxin (baseline, black), presence of toxin alone (maroon), and toxin mixed with *E. reginae* liver extract (orange). Current recovery with liver-treated toxin relative to baseline and toxin alone, for *E. reginae* liver (orange), *C. tenuis* liver (teal), and mouse liver (blue). Each point represents a single cell (n = minimum of 4 cells) and error bars represent standard deviation (SD). Asterisks represent statistically significant differences in toxin current recovery between extracts ($p < 0.0001$, one-way ANOVA with Tukey's post hoc test).

High expression of transporter-related proteins in the liver is associated with *A. trivittata* consumption by *E. reginae*

Following prey ingestion, it is expected that digestive enzymes are upregulated. However, in the case of toxic prey, such as *A. trivittata*, we hypothesized that additional detoxification mechanisms would also be activated. To test the hypothesis that specific molecular candidates mediate the detoxification cascade from ingestion through digestion, we generated transcriptomes from four digestive tissues (tongue, stomach, liver, and gut) in *E. reginae* individuals that had consumed *A. trivittata* ($n = 3$), *Scinax ruber* ($n = 3$), or were fasting ($n = 3$) (Table S2). Transcriptomes clustered primarily by tissue, with the tongue showing the most distinct expression profile (Fig. S6A–B). Across pairwise comparisons, the greatest number of differentially upregulated genes was observed in response to *A. trivittata* consumption, with the liver showing the strongest transcriptional response among the tissues (Fig. 3A–B). In contrast, *S. ruber* elicited the weakest transcriptional activation across tissues. Fasting snakes show upregulation of certain genes, particularly in the stomach. In other studies, gene upregulation in the digestive tissues of hibernating animals has been linked to increased sphingolipid metabolism (Wei et al. 2025).

As liver extracts from fasting *E. reginae* individuals were able to neutralize *A. trivittata* toxin block of *HsNa_v1.4* expressed in mammalian cells, we therefore investigated the liver transcriptome, expecting to identify candidate genes encoding soluble proteins capable of toxin binding. Since no detergents were used during either the protein extraction or toxin incubation in the liver neutralization assay, it likely primarily captured soluble candidate proteins while excluding membrane proteins. Literature suggests several soluble proteins may contribute to toxin neutralization, including serpins (Alvarez-Buylla et al. 2023), transferrin-like proteins (*TF*, *TFRC*, *TFR2*, *TFIP11*) (Barabas and Faulk 1993; Tortorella and Karagiannis 2014), and lactotransferrin-like proteins (LOC139173594) (Ruiz-Mazón et al. 2024). However, only one of these genes in one treatment showed significant upregulation (adjusted p -value < 0.05): *SERPIN6* in the liver of snakes fed *S. ruber* (Fig. S6C). Gene Ontology (GO) enrichment analysis (TopGO, cellular component category) did not detect enrichment of soluble proteins (Fig. S6D). Nonetheless, the soluble proteins that could contribute to toxin neutralization were all expressed in the transcriptomes, suggesting their presence in the liver even without differential upregulation in response to fasting or eating. Thus, given that the neutralization assay was conducted on liver tissue from fasting individuals, these results suggest that presence, rather than overexpression, of toxin-binding proteins may be sufficient for functional resistance. Furthermore, some toxin-binding proteins may remain uncharacterized, potentially corresponding to unannotated LOC genes that were upregulated (see Dataset S3) (Alvarez-Buylla et al. 2023).

Focusing on liver-specific responses to consumption of *A. trivittata*, GO enrichment (TopGO, molecular function category) (Alexa and Rahnenfuhrer 2022) revealed a significant overrepresentation of genes involved in transport activity (Fig. 3C). Among the most upregulated were members of the solute carrier (SLC) family, which are widely known for their roles in the absorption, uptake, and clearance of xenobiotics and drugs (Nigam 2015; Pizzagalli et al. 2021) (Fig. S6C). For example, the upregulated gene *SLC22A7*, in humans, encodes a known organic anion transporter involved in hepatic excretion of toxins and metabolites, including the plant and amphibian pyrrolizine toxins (Enge et al. 2021; Pizzagalli et al. 2021; Waizenegger et al. 2021). Other upregulated solute carriers included *SLC15A1*, involved in peptidomimetic uptake (Kawai et al. 2020), and transporters such as *SLC1A5*, *SLC16A6*, and *SLC5A12*, linked to amino acid and monocarboxylate metabolism (Pizzagalli et al. 2021). While many of these transporters exhibit substrate overlap and species-specific variability, their roles in xenobiotic handling make them strong candidates for contributing to toxin clearance (Nigam 2015). This multifunctionality of SLC transporters warrants further investigation, especially considering that non-synonymous mutations in SLC genes have been linked to altered substrate specificity and transporter efficiency (Han et al. 2011; Engström et al. 2013; Yee et al. 2013). Such mutations may underlie evolutionary adaptations that enable predators like *E. reginae* to regularly consume chemically defended prey without succumbing to their most toxic effects.

Other proteins involved in transport were also overexpressed in *E. reginae* after consumption of *A. trivittata*. These include ABCA12 and NPC1L1, known lipid and cholesterol transporters (Peelman et al. 2003; Jia et al. 2011). Given their role in lipophilic molecule transport, these proteins may contribute to the movement of hydrophobic toxins such as HTX and PTX. The upregulated RAB11FIP1, a protein involved in the regulation of intracellular transport vesicles, may play a role in facilitating toxin engulfment, intracellular trafficking, and eventual elimination, potentially contributing to the cellular handling of toxic compounds (Damiani et al. 2004).

Beyond direct detoxification, transporters also play essential roles in maintaining systemic homeostasis. Their increased expression in response to *A. trivittata* ingestion may reflect a broader metabolic stress response, involving inter-organ signaling and physiological adaptation rather than toxin elimination alone (Nigam 2015). Supporting this idea, we observed overexpression of heat shock proteins, including HSPA2 and its associated regulator HSPBAP1, in snakes following *A. trivittata* consumption (Feder and Hofmann 1999) (Fig. S6C). The phospholipase PLA2G7, a gene found in the venom of various organisms such as snakes, bees, and scorpions, as well as the sphingosine-1-phosphate plasma transporter *MFSD2B*, were also highly expressed and are known to be involved in inflammatory responses (Vu et al. 2017; Spolaore et al. 2019; Li et al. 2021; Candels et al. 2022; Le et al. 2022) (Fig. S6C). These proteins are well-established markers of cellular stress and may signal a generalized physiological response to toxic prey ingestion.

Altogether, our RNA-seq data suggest that transporter overexpression in the liver represents a complementary resistance mechanism, likely supporting toxin elimination rather than direct neutralization. While no previously reported toxin-binding proteins were strongly upregulated after *A. trivittata* consumption, the presence of soluble candidates and upregulation of transmembrane transporters indicate that multiple pathways, including toxin binding, membrane trafficking, and metabolic elimination, jointly contribute to toxin resistance in *E. reginae*.

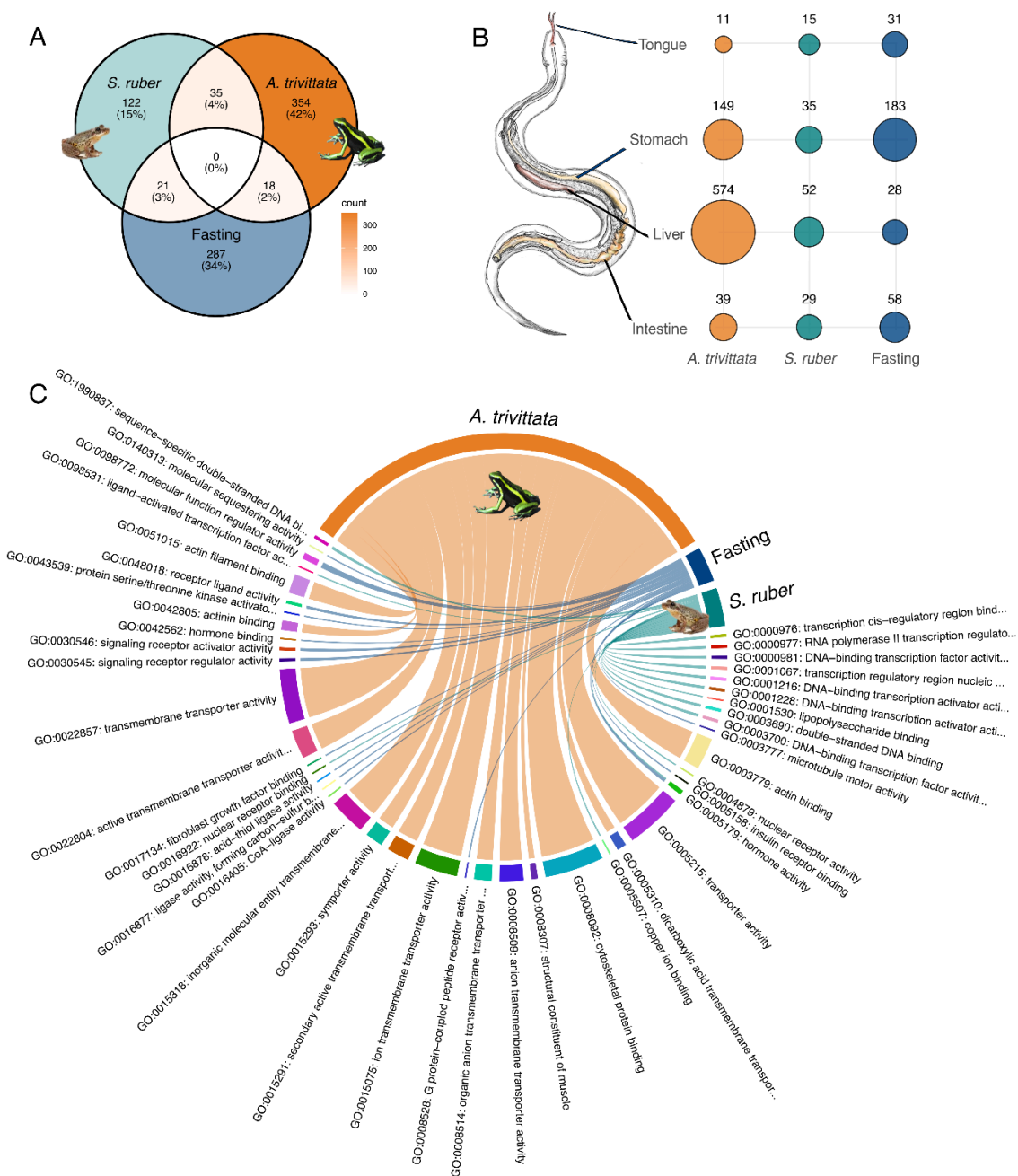


Figure 3. Consumption of *A. trivittata* changes liver gene expression in *E. reginae* more than in other conditions and induces high expression of transporter genes. (A) Venn diagram showing the overlap of upregulated protein-coding transcripts across three conditions after differential expression analysis between fasting vs. *A. trivittata*, fasting vs. *S. ruber*, and *S. ruber* vs. *A. trivittata* of the combined digestive system tissues (tongue, stomach, liver, and intestine). (B) Number of upregulated protein-coding transcripts in each digestive tissue after differential expression analysis between fasting vs. *A. trivittata*, fasting vs. *S. ruber*, and *S. ruber* vs. *A. trivittata*. Snake diagram was drawn by Bernardo Moreno Peniche. (C) Circular plot representing the upregulated liver Gene Ontology (GO) enrichment analysis (molecular function

category) using topGO in *E. reginae* across the three conditions. Each segment represents a GO term, labeled with its molecular function. The width of each segment corresponds to the "Significant" value, indicating the number of upregulated genes associated with each GO term.

Some *E. reginae* muscular voltage-gated sodium channel alleles (Na_v1.4) are highly resistant to tetrodotoxin, saxitoxin, and neo-saxitoxin

The final frontier of toxin resistance is the toxin target itself. If the toxin reaches its ultimate target, amino acid substitutions in the target protein can lower its affinity or prevent toxin binding altogether—a mechanism known as target-site resistance (TSR) (Geffeney et al. 2005; Catterall 2014; Ujvari et al. 2015; Marquez et al. 2017; Tarvin et al. 2017; Abderemane-Ali et al. 2021; Mohammadi et al. 2021; van Thiel et al. 2022). Putative TSR mechanisms have been previously identified in gene sequences of *Erythrolamprus* snakes (Feldman et al. 2012; Ramírez-Castañeda et al. 2024). In some *E. reginae* populations, Na_v channels exhibit amino acid substitutions at sites experimentally reported to confer tetrodotoxin (TTX) resistance in Na_v1.1, Na_v1.3, Na_v1.4, Na_v1.6, and Na_v1.8 (Terlau et al. 1991; Geffeney et al. 2005; Vaelli et al. 2020; Ramírez-Castañeda et al. 2024). Additionally, bufadienolide-resistance-associated amino acid changes have also been observed in the *ATP1A3* sodium-potassium pumps which could potentially explain its ability to feed on frogs containing cardiac glycosides, such as *Rhinella margaritifera* (Mohammadi et al. 2016).

The evolution of TSR in the muscle-expressed Na_v1.4 sodium channel is closely associated with toxin resistance in organisms exposed to high levels of neurotoxins such as TTX and STX (Ramírez-Castañeda et al. 2024). However, physiological experiments are necessary to confirm whether amino acid substitutions linked to TSR actually alter toxin sensitivity or affect protein function (Abderemane-Ali et al. 2021). We tested the hypothesis that TSR-associated mutations in *E. reginae* Na_v1.4 reduce channel sensitivity to guanidinium neurotoxins. To do so, we examined two variants: a putative resistant variant (R) that harbors TTX TSR-associated mutations and a non-resistant variant (NR) from populations lacking these mutations, as described in Ramírez-Castañeda et al. (2024) (Fig. S1, Dataset S4).

The resistant *E. reginae* Na_v1.4 variant includes five amino acid substitutions at functionally relevant sites (Fig. S1), and at least two of them, D1539N and G1540D, have been characterized in other species as TTX resistance-conferring changes (Geffeney et al. 2005; Mc Glothlin et al. 2014; Vaelli et al. 2020). Using two-electrode voltage-clamp (TEVC) recordings in *Xenopus laevis* oocytes, we compared the toxin responses of the resistant (R) and non-resistant (NR) *E. reginae* Na_v1.4 variants, alongside the human Na_v1.4 (*HsNa_v1.4*) channel as a control. These recordings, performed under single-stimulus protocols, allowed us to assess the extent to which the resistant variant contributes to toxin resistance in *E. reginae*. Importantly, we expressed the wild-type *E. reginae* Na_v1.4 channel rather than introducing point mutations into a model organism, preserving natural channel variation and its full response to toxin exposure. To provide a comprehensive characterization of the *ErNa_v1.4* resistant (R) and non-resistant (NR) variants, we evaluated basic electrophysiological properties such as activation and inactivation curves (Fig. S8), the half-maximal activation and inactivation voltages (V_{activation,1/2} —*ErNa_v1.4* (R): -XXX mV ± XXX mV, (NR): -XXX mV ± XXX mV; V_{inactivation,1/2} —(R): -52.47 ± 2.929, (NR): -53.32 ± 3.229) (Fig. S8 and Table S5). Inactivation curves showed no differences between the two variants, suggesting that the substitutions distinguishing both do not affect these channel properties, consistent with previous findings (Carlo et al. 2024).

We first conducted concentration–response curves for each toxin and identified that the IC_{50} values for *ErNa_v1.4* (R) are extremely high, in some cases, even the highest toxin concentrations applied had negligible effect on channel activity, making the precise IC_{50} calculation not possible (Fig. 4, *ErNa_v1.4* (R) TTX & STX $IC_{50} \gg 3000$ nM; neoSTX $IC_{50} \gg 333$ nM; Fig. 3). In contrast, *ErNa_v1.4* (NR) exhibited a sensitivity profile closely aligned with that of *HsNa_v1.4*, with the following rank order: neoSTX > STX > TTX (Fig. 3, IC_{50} 0.4048 nM \pm 0.235 nM, 6.565 nM \pm 1.013 nM, and 18.09 \pm 2.02 nM, respectively). IC_{50} values for *HsNa_v1.4* are reported in Table S4. These results demonstrate that target-site resistance (TSR) in *ErNa_v1.4* (R) is the primary mechanism conferring high resistance to TTX, STX, and neoSTX in *E. reginae*.

While five amino acid substitutions are present in the *E. reginae* Na_v1.4 resistant variant, not all are likely to contribute equally to the observed resistance. The substitutions D1539N and G1540D, located in the domain IV p-loop (selectivity filter), are well-characterized TSR mutations previously shown to confer high TTX resistance (Geffeney et al. 2005; McGlothlin et al. 2014; Vaelli et al. 2020), and likely represent the primary contributors to the STX and TTX-resistant phenotype in *E. reginae* as shown in the structural models (Fig. 4M–P). An additional substitution, P1550S, also occurs in this region and is found in dendrobatid frogs, though its functional role remains unclear. Structural modeling (Fig. 4M–P) shows that the remaining substitutions, I425L (domain I, segment 6) and S725N (domain II, segment 5), are located on the outer face of the pore domain, making it unlikely that they directly affect STX or TTX binding. Notably, S725N is also found in highly TTX-resistant species such as *Heterodon platirhinos* and *Thamnophis sirtalis* (Willow Creek population), despite not being previously identified as a TSR site (Feldman et al. 2016; Ramírez-Castañeda et al. 2024). Together, these data suggest that while five substitutions are present, resistance is most parsimoniously explained by the convergent D1539N and G1540D mutations in the domain IV p-loop, consistent with findings from other resistant lineages (Geffeney et al. 2005; Vaelli et al. 2020). Nomenclature is based on the human Na_v1.4 sequence.

These toxins are common across various ecosystems but have not yet been documented in the known diet or habitat of *E. reginae* (Ramírez-Castañeda et al., 2024). The extreme resistance observed in some individuals suggests that populations of *E. reginae* may be exposed to high concentrations of one or more of these toxins (Pearson & Tarvin, 2022; Ramírez-Castañeda et al., 2024). Because GC–MS cannot detect TTX, its presence in *A. trivittata* cannot be ruled out. Interestingly, neoSTX appears to be counteracted by two independent resistance mechanisms: liver-expressed proteins that neutralize the toxin (Fig. 2F) and TSR-associated mutations in Na_v1.4. Although we initially hypothesized that this redundancy evolved in response to the extreme potency of neoSTX ($IC_{50} < 1$ nM), STX is also a low-nanomolar blocker, making a strictly potency-based explanation less conclusive. Moreover, the added protection conferred by liver-mediated detoxification, despite the strong TSR-mediated resistance, raises the possibility that neoSTX may have an additional, unidentified molecular target.

Our findings confirm the coexistence of multiple resistance mechanisms in an Amazon Basin population of *E. reginae* from Leticia, Colombia. This population carries the *ErNa_v1.4* (R) variant and was also the source of liver samples used in recovery assays demonstrating the capacity to neutralize dendrobatid toxins and neoSTX (Dataset S5). Together, these results indicate that this population exhibits both target-site resistance in Na_v channels and liver-mediated detoxification, highlighting the integrative nature of toxin resistance in this species and its ability to counteract complex chemical defenses.

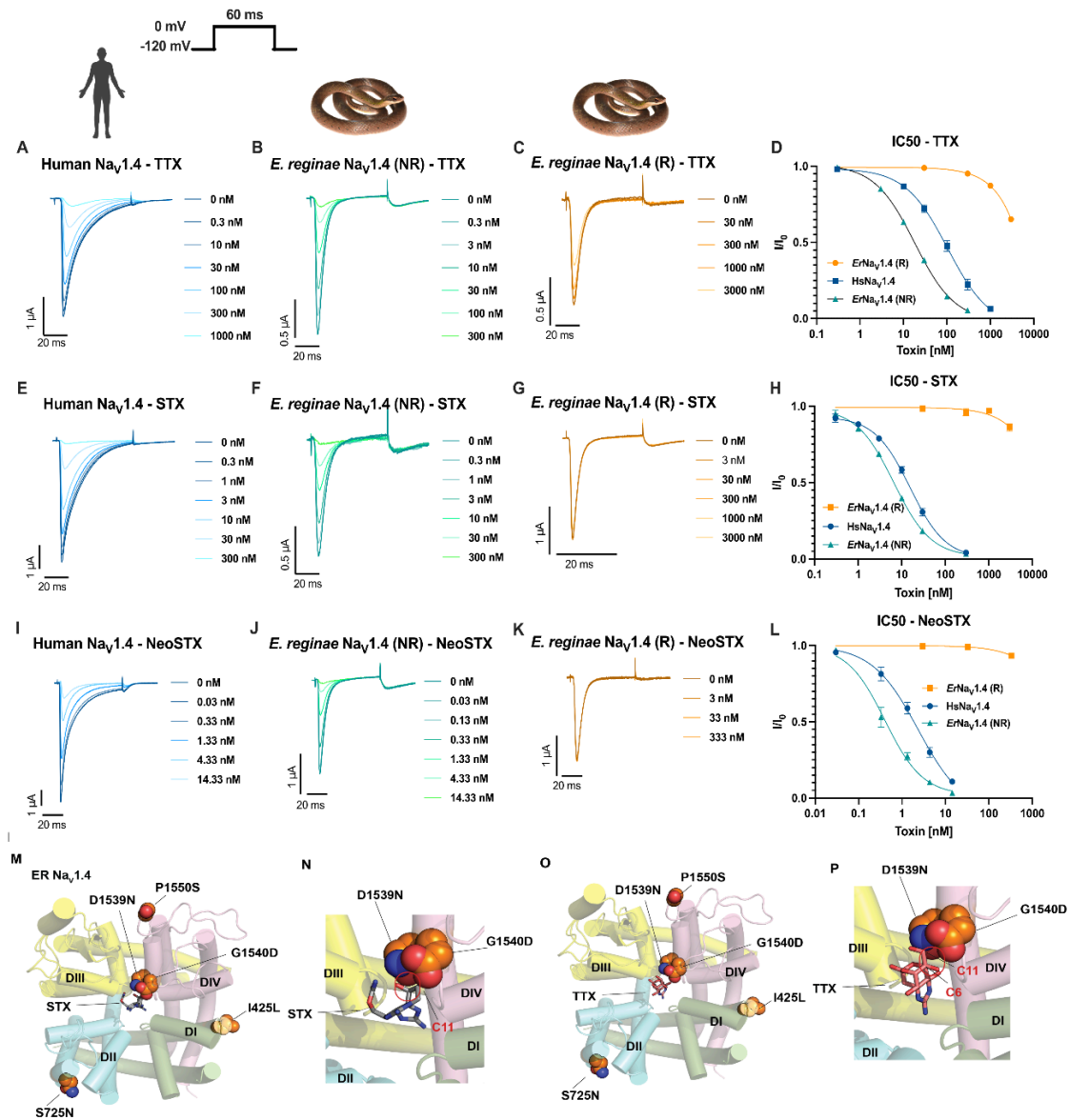


Figure 4. Amino acid substitutions in the *E. reginae* $\text{Na}_V1.4$ (R) variant confer high resistance to the neurotoxins TTX, STX, and neoSTX. Exemplar recordings for Human $\text{Na}_V1.4$ (*HsNa_V1.4*, blue), *E. reginae* $\text{Na}_V1.4$ non-resistant variant (*ErNa_V1.4* (NR), green), and *E. reginae* $\text{Na}_V1.4$ resistant variant (*ErNa_V1.4* (R) in orange) expressed in oocytes were exposed to increasing concentrations of TTX (A, B, C), STX (E, F, G) and neoSTX (I, J, K). Concentration-response curves were subsequently plotted for each Na_V channel for TTX, STX, and neoSTX (D, H, L; respectively; for values, see Table S4). Each point represents mean normalized current with standard deviation ($n = 6$). Note the different toxin concentrations used for *ErNa_V1.4* resistant variant (C, G, and K) compared to other graphs. Structural interactions of STX (M, N) and TTX (O, P) with a model of the *E. reginae* $\text{Na}_V1.4$ resistant variant. Residues shown in space-filling representation highlight the five amino acid substitutions at functionally relevant sites that differentiate the resistant from the non-resistant *ErNa_V1.4*. Among these, only

D1539N and G1540D appear to interact directly with the guanidinium toxins. Residue numbers correspond to the position in Human Na_v1.4.

***E. reginae* Na_v1.4 (R) is sensitive to *A. trivittata* secreted toxins**

Na_v1.4 has been identified as a key target of several toxins secreted by *A. trivittata*, including HTX and PTX (Daly 1995; Santos et al. 2016). To test the hypothesis that TSR-associated mutations in Na_v1.4 confer resistance to specific toxins present in *Ameerega* frogs, we exposed *E. reginae* channels to various toxins, including *A. trivittata* skin secretions, using *S. ruber* skin secretions as a control. We also tested isolated compounds found in *Ameerega* species, including histrionicotoxins (HTX293A and H₈-HTX), pumiliotoxins (PTX251D), and decahydroquinolines (DHQ167 and DHQ195A).

We therefore assessed whether the amino acid substitutions in the *Er*Na_v1.4 resistant variant also conferred resistance to naturally occurring dendrobatid toxins by TEVC recording. Due to the scarcity of toxin material, we only used the *Hs*Na_v1.4 as the control channel, as it is regularly used as a model organism, and only assessed a single high toxin concentration that allowed for sufficient repetitions to ensure statistical robustness in both the resistant and human channels.

Unexpectedly, the *Er*Na_v1.4 (R) channel did not exhibit resistance to the skin secretions of its toxic prey, *Ameerega trivittata*, with a ~20% reduction of the current and showed only a slight ~5% reduction in current when exposed to *S. ruber* secretion (Fig. 3C: *Er*Na_v1.4 (R) *A. trivittata* secretion, significant reduction; Kruskal-Wallis test, $P \leq 0.01$; Fig. 3F: *Er*Na_v1.4 (R) *S. ruber* secretion, Kruskal-Wallis test, $P \leq 0.01$). Although not statistically significant, the human channel showed a ~10% reduction in current following exposure to *A. trivittata* secretions. To further validate these findings, we tested individual toxins found in *A. trivittata* and other dendrobatid frogs, including the alkaloids noted above (Fig. S7). Consistent with the whole-secretion current reductions, neither the *Er*Na_v1.4 (R) nor the human control channel exhibited resistance to any of these toxins ranging from ~10%-60% current reduction (significant reduction; Kruskal-Wallis test, $P \leq 0.05$). These findings suggest that *E. reginae* relies on alternative toxin resistance mechanisms, such as metabolic transportation for detoxification and elimination or target-binding proteins, to consume *A. trivittata*, as discussed in previous sections. However, we cannot rule out the possibility that TSR plays a role in other ion channels, given that some *A. trivittata*-derived toxins are known to target channels beyond Na_v1.4, such as nicotinic acetylcholine receptors (Daly REF; Santos et al., 2016). Additionally, the concentrations used in this study for some of these toxins (Table S3) are exceedingly high compared to those typically encountered in nature, further suggesting that Na_v1.4 may not be the primary target of some of these toxins, as mentioned in previous sections (Jeckel et al. 2015; Jeckel et al. 2019; Lawrence et al. 2019). Overall, our results indicate that TSR in *Er*Na_v1.4 is not the primary resistance mechanism against *A. trivittata* secretions but is essential for resistance to TTX-, STX-, and neoSTX-secreting prey.

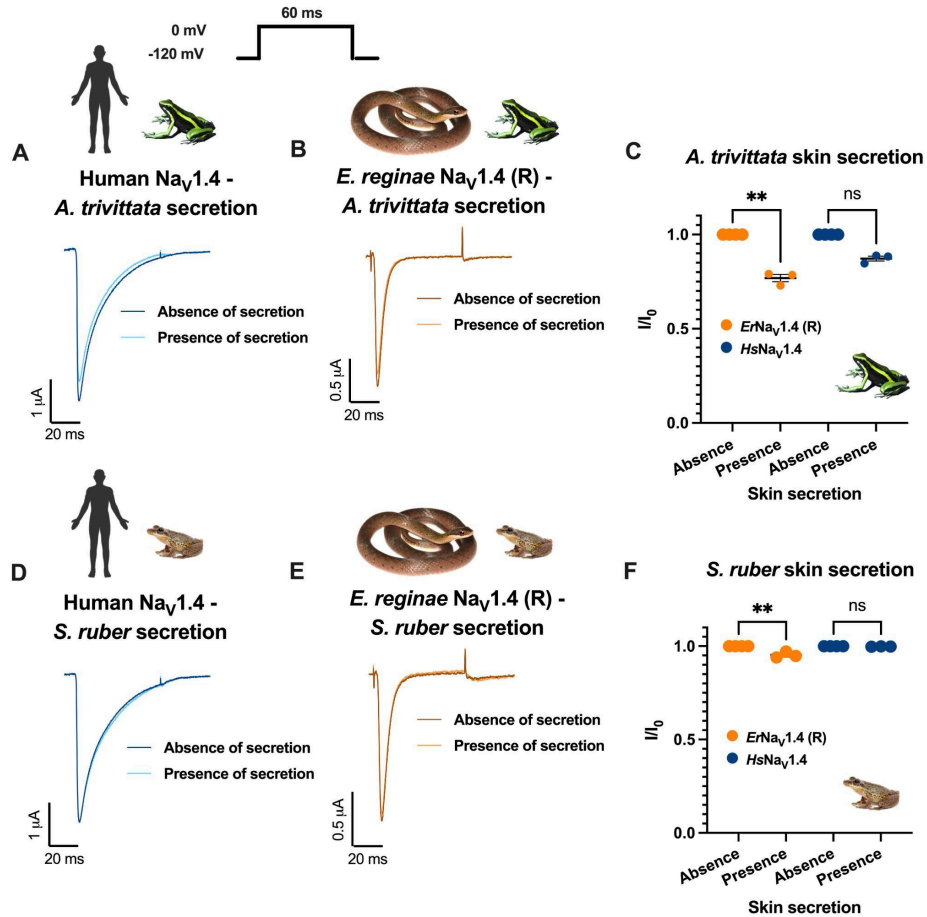


Figure 3. *E. reginae* $\text{Na}_V1.4$ (R) is sensitive to the *A. trivittata* poison frog skin secretions. Exemplar current recordings for Human $\text{Na}_V1.4$ ($\text{HsNa}_V1.4$ in blue) and *E. reginae* $\text{Na}_V1.4$ resistant variant ($\text{ErNa}_V1.4$ (R) in orange) expressed in *X. laevis* oocytes and exposed to 1:1000 dilution of reconstituted skin secretions from *A. trivittata* (A and B) or *S. ruber* (D and E). Comparison of sodium current reduction in the presence or absence of *A. trivittata* (D) and *S. ruber* (F) skin secretions. Statistical significance was assessed using a Kruskal-Wallis test, with p-values provided for the corresponding comparisons. P-values are shown in the graph as (ns) $P > 0.05$; (*) $P \leq 0.05$; (**) $P \leq 0.01$; (***) $P \leq 0.001$.

Conclusions

This study demonstrates that toxin resistance in *Erythrolamprus reginae* is not the result of a single trait but instead emerges from a multi-scale and dynamic integration of behavioral, physiological, and molecular adaptations. By investigating toxin resistance strategies at distinct stages—prey selection and handling, detoxification during digestion, and molecular insensitivity at the toxin's target—we reveal how predators overcome diverse chemical defenses through complementary strategies. Our findings contribute to a broader understanding of how resistance evolves in chemically complex environments and how it may reshape organismal physiology.

To understand how *E. reginae* copes with toxic amphibian prey, we tested several interrelated hypotheses. We showed that *E. reginae* exhibits longer handling times and aversive behaviors toward the highly toxic *A. trivittata* compared to the non-toxic *S. ruber*, suggesting that prey toxicity imposes handling costs that may influence foraging decisions. Due to this aversion, further research is necessary to investigate the physiological and ecological factors that could drive a snake to feed on a poisonous frog, considering, for example, that not all of our snakes survived following the predation event. Moreover, seasonal changes like dry and flood periods could affect prey availability and foraging choices.

We also developed a novel assay that revealed that soluble proteins in the liver can partially restore sodium channel activity inhibited by *A. trivittata* alkaloids and neoSTX, supporting the presence of toxin-binding proteins that contribute to detoxification. These results demonstrate an ecologically specific soluble protein response to *Ameerega* alkaloids observed in *E. reginae*, but not in another colubrid snake from a different ecosystem. Transcriptomic profiling across tissues identified liver-specific upregulation of transporter genes, such as those in the solute carrier family, and stress-response genes following exposure to *A. trivittata*. This indicates that transporter expression may represent a complementary mechanism of toxin elimination in the liver, alongside the toxin-binding proteins.

Electrophysiological recordings confirmed that one of the *E. reginae* voltage-gated sodium channel *ErNa_v1.4* allele is highly insensitive to TTX, STX, and neoSTX, demonstrating that TSR mutations confer robust molecular resistance to some but not all prey alkaloids. These results highlight a dual resistance mechanism for neoSTX and also raise questions about which prey items may be exposing these snakes to TTX, STX, and neoSTX, which are compounds not yet reported in Amazon forest frogs except for the rare Harlequin frogs (genus *Atelopus*), which have TTX. The same TSR mutations in *ErNa_v1.4* did not prevent inhibition by *A. trivittata* alkaloids, suggesting that resistance to these toxins depends on alternative targets or mechanisms, such as the toxin-binding or transporter proteins described in this study. Looking forward, further research should investigate additional molecular targets of frog alkaloids to clarify these alternative resistance pathways.

Collectively, our results highlight that *E. reginae* employs a layered resistance strategy, relying on behavioral aversion, detoxification, and sodium channel insensitivity. The coexistence of TSR and liver-based mechanisms in the same population suggests that *E. reginae* populations may be adapting to a chemically diverse diet by evolving multiple, overlapping forms of resistance. These findings underscore the complexity of toxin resistance, where selection may favor multiple mechanisms acting at different physiological levels to mitigate the effects of prey toxins. Future studies building on these results could provide insights into the ecological and physiological trade-offs associated with these resistance mechanisms. Comparative population genomics across additional *E. reginae* populations, especially those with varied dietary exposures, could reveal how local selection shapes the evolutionary dynamics of toxin resistance alleles. Such future directions will refine our understanding of the evolution of complex traits and contribute to unraveling the multiple biological scales involved in the resistant phenotype.

Acknowledgments

We thank the Russell E. Train Education for Nature Program (EF14103) from the World Wildlife Fund (WWF), the National Institutes of Health (NIGMS #R35GM150574 to RDT, NIGMS 1S10GM154292-01 to RWF), National Science Foundation (DUE-0942345, IOS-1556982 to RWF), the MVZ Wake Research Award, and the GRAC Research Funds from the Integrative Biology Department at UC Berkeley, which supported VRC's expenses during field collection, analysis, and writing. This work was partially supported by grants DoD HDTRA-1-19-0040, HDTRA-1-21-1-0011, and HDTRA-1-23-0026 to DLM. Thanks to José Rances Caicedo Portilla and Martha Calderón for all your help during the animal collection process. We are very grateful to all the members of the Minor Lab and the Tarvin Lab for their help during the electrophysiology experiments, and to the EGL Laboratory and QB3 Genomics, especially Lydia Smith, for your dedicated support during the transcriptome library preparation. We thank J. Du Bois for supplying STX samples. Special thanks to José Guillermo Díaz Cahuachi, Ana Milena Castro, Francly Silva, the Kuiru family (Mirna Kuiru, Luna, Marco, and Camila), and the Naforo-Bautista family (Maritza Naforo Bautista, María Bautista Pinto, Juan Naforo Bautista, Orfilia Gomez, Velentina) for your knowledge, kindness, and invaluable help during sample collection, predation experiments, and in general, for making this research possible. We thank Reserva Maiku in Puerto Nariño and the Hermanos Menores Capuchinos de Leticia for granting us permission to work on their lands. We are deeply grateful to all the local guides and workers who assisted us and generously shared their time and knowledge. We are also thankful for the opportunity to observe and interact with snakes and frogs, to witness them up close, and to share a home with them, the forest, and the cities where they live. The Spanish translation was produced using ChatGPT and edited by VRC (Available in Dataset S7) (OpenAI, 2023).

Methods

Animal collection

We collected 12 *Erythrolamprus reginae* snakes, 6 *Ameerega trivittata* frogs, and 6 *Scinax ruber* frogs from Leticia, Amazonas, Colombia (Table S1). These specimens were captured by hand or using a snake hook. Collection permit was granted by the Colombian Authority for Environmental Licenses (ANLA; No. 1249, 23 July 2020, RCI0002-00-2020). To avoid any impact of chemical euthanasia on our results, we euthanized snakes by decapitation followed by rapid extraction of the brain tissue. Frogs were euthanized using hypothermic shock. Euthanasia and predation trial (below) protocols were approved by the IACUC No. AUP-2019-08-12457-1 issued by the University of California Berkeley, USA. Non-CITES tissue samples were exported under the ANLA permits No. 02191, No. 02376, and No. 3271. For *A. trivittata* the exportation of the tissues was granted by the CITES export permits No. CO26165 and No. CO46959.

Predation Behavior Test

We hand or snake-hook captured snakes and housed them individually close to the site of capture in mesh cages (30 cm x 30 cm from RestCloud) with water, and natural leaves, ground, and hiding spots (log cylinders) for an acclimatization period of five days. This period ensured that the digestive tracts of the snakes were empty before the experiment. The anurans were collected one or two days before each trial and kept under the same mesh cages conditions. We video-recorded using a Nikon D5600 camera *E. reginae* predation events against the poisonous frog *A. trivittata* (Dendrobatidae) and the non-poisonous *S. ruber* (Hylidae; Dataset S1 & Dataset S2). If after 2 hours the toxic frog was not ingested, we removed the toxic frog, and a second frog—*Leptodactylus* sp., *Sphaenorynchus lacteus*, *Dendropsophus* sp., *Rhinella margaritifera*, or *Scinax ruber*—was introduced to the enclosure to determine whether the snake was generally unwilling to eat or specifically rejected *A. trivittata* (see Fig. 1A). All offered frogs are natural prey of *E. reginae*, ensuring that the experiment simulated natural feeding conditions.

During the experiment, the snake and posteriorly the frog were introduced into an empty mesh enclosure. We recorded the interaction until 40 minutes after ingestion or vomiting of the frog, or up to two hours if no ingestion occurred. If no predation was observed, the trial was terminated after two hours. Predation events were classified as "ingested," "vomited," or "avoided" following Brodie and Tumbarello (1978). Snakes were euthanized 40 minutes after the frog was completely swallowed to obtain tissue samples for transcriptome analysis. According to (Williams et al. 2010), toxin intoxication effects become measurable within 30–40 minutes post-ingestion. Video recordings were analyzed to document notable behaviors, including the time elapsed from the first attack to the moment the frog was fully swallowed ("Time to swallow") and the number of times the snake exhibited dragging behavior ("Dragging cycles"). We define dragging behavior as the act of swabbing or rubbing the frog, already held in the snake's mouth, along the floor or wall. Each dragging cycle was counted from the moment the snake began dragging to when it paused, rather than based on the number of physical drags performed.

Transcriptome

RNA library preparation

Snakes were sacrificed after each predation experiment (*A. trivittata* or *S. ruber* ingestion) or after a 5-day fasting period (control; Table S2). Snake tissues were collected in the field, stored in RNA later, and transported for a longer storage at -80 °C freezer (Table S2). For RNA extraction, we used the Monarch® Total RNA Miniprep Kit from NEB Biolab and followed the protocol for <10 mg initial tissue. The homogenization of the tissues was performed using the PowerLyzer™ 24 bead beater (MO BIO Laboratories, Inc.), with two cycles of 3500 RPM for 45 seconds, each followed by a 30-second rest period, and an intermediate speed of 3500 RPM. To assess starting RNA quantity and quality, we used the Qubit RNA HS Assay Kit from ThermoFisher Scientific and Bioanalyzer RNA Analysis from Agilent.

For the RNA library prep, we selected the high quality RNA samples (RIN \geq 7) with up to 500 ng RNA, except for a few irreplaceable samples that had low RIN scores despite several extraction attempts. We followed a poly(A) selection protocol for all samples using the Watchmaker mRNA Capture Kit from Watchmaker Genomics. For the library amplification, seven extra cycles were used for the low RIN score samples (Table S2). RNA libraries were sequenced to obtain ~30 M paired-end reads (150 bp) per tissue on a Illumina NovaSeq™ X 10B flow cell. Raw data is available in (Bioproject PRJNA1274516, see complete biosample numbers in table S1).

RNA-seq data processing and analysis

Raw paired-end RNA-seq reads were quality-filtered and trimmed using fastp v0.23.2 (Chen et al. 2018; Chen 2023) with adapter detection enabled and default settings. Cleaned reads were aligned to the *E. reginae* reference genome (GCF_031021105.1) using HISAT2 v2.2.1 (Kim et al. 2015) with the *--dta* flag to facilitate transcript assembly. Alignment outputs in SAM format were converted to BAM, sorted, and indexed using Picard and samtools v1.21. Alignment quality metrics were generated with the *flagstat* tool. The genome annotation file (GFF) was converted to GTF format using gffread (Pertea and Pertea 2020), with manual correction of gene identifiers to ensure compatibility with downstream quantification tools. Transcript abundance was quantified using HTSeq-count v0.13.5 (Putri et al. 2022) in unstranded mode (*-s no*) with exon-level features and gene-level aggregation (*-i gene_id*).

Transcript abundance data were analyzed using DESeq2 in R (v4.3.0) (Love et al. 2014). Count matrices from HTSeq-count were merged and filtered to include genes expressed in digestive tissues: liver, tongue, stomach, and intestine. These tissues were obtained from 3 different feeding treatments (see above): after 5 days fasting, or 40 minutes after the ingestion of an *A. trivittata* or *S. ruber* prey. Differential gene expression (DE) analyses were performed using DESeq2 with tissue and condition as covariates (see dataset S3: log₂fold and p-value results). Principal component analysis (PCA) and volcano plots were generated to assess sample clustering and DE genes (Fig. S7). Genes with adjusted p-value < 0.05 and log₂FoldChange > 0 were considered significant and upregulated (Dataset S3). The final list of upregulated genes for each condition was compiled by combining DE genes identified across the three pairwise comparisons: fasting vs. *A. trivittata*, fasting vs. *S. ruber*, and *S. ruber* vs. *A. trivittata*. For the expressed gene counts, we retained only protein-coding genes from the set of upregulated transcripts by filtering the set of upregulated genes by *E. reginae* gene identifiers from the NCBI genome annotation classified as protein-coding. To investigate functional patterns of gene expression across conditions, we classified differentially expressed genes into biologically relevant categories based on gene name patterns and annotations. Using regular expressions, we extracted gene sets associated with specific protein families and functional categories from the differential expression results.

Gene categories related to toxin resistance were used to highlight potential differential expression of these genes in the volcano plots (Fig. S7). We grouped solute carrier family genes (SLC), phospholipase A2 genes (PLA2), cytochrome P450 genes (CYP), serine protease inhibitors (SERPIN), ATP-binding cassette transporters (ABC), heat shock proteins (HSP), and Rab GTPases (RAB) based on their gene name prefixes. Transferrin-related genes (TF, TFRC, TFIP11, and TFR2) were grouped using known gene symbols. Cholinesterase-like genes (*E. reginae* transcript IDs: LOC139158370–LOC139158371, LOC139159376, LOC139160160, LOC139160166, LOC139160209–LOC139160211, LOC139160214–LOC139160215, LOC139160217, LOC139160219–LOC139160220, LOC139160232), lactotransferrin-like gene (ID: LOC139173594 and LTF) and 85 transporters genes (table S6) were manually identified using the ncbi gene annotations of *Erythrolamprus reginae* (GCF_031021105.1).

Functional enrichment of DE genes was assessed using topGO (ontology: Molecular Function) (Alexa and Rahnenfuhrer 2022). Gene-to-GO mappings were obtained using *Anolis carolinensis* annotations (Unitprot taxon ID 28377). Only genes with detectable expression across samples (mean normalized counts > 0.5) were used as background. Enrichment results were visualized using the molecular function option “MF” and cellular component option “CC”.

Skin secretion GC-MS toxin profile analysis

Following euthanasia, we removed entire skins from 6 *A. trivittata* and 6 *S. ruber* and placed each in ~1 mL 100% ethanol in glass vials with PTFE-lined caps and stored at -80 °C. A 100 µL aliquot of the solution was sampled and analyzed directly by Gas-Chromatography Mass-Spectrometry (GC-MS). Samples (1 µL) were analyzed using either a Thermo iTQ1100 unit resolution ion trap instrument or Thermo Exploris GC high-resolution orbitrap instrument. GC separation used 5% phenyl methylsilicone columns (Restek RTX-5MS or Thermo TG-5Si, 0.25 mm x 30m, 0.25 µm film thickness) with splitless injection with a ramp from 100C to 280C as previously described. Retention indices (Kovats) were determined by comparison to alkane standards injected with the group. Samples were sequentially analyzed in electron ionization (EI) and chemical ionization with ammonia reagent gas (CI-NH₃). Compounds were identified by comparison with EI library spectra, molecular weight/formula match and retention index.

Electrophysiology

Toxin sources and preparation for electrophysiology analyses

STX was synthesized as described (Andresen and Bois 2009). Neosaxitoxin (neoSTX) was purchased from Sigma Aldrich (Sigma-Aldrich GmbH, Switzerland, cat. no. 41619). Tetrodotoxin citrate (TTX) was purchased from Cayman Chemical (MI, USA, cat. no. NC1735928). All toxins were lyophilized and dissolved in ultrapure water in stocks of 1–5 mM for further use.

From the original 100% ethanol solution containing whole-skin extracts of *A. trivittata* and *S. ruber*, 100 µl was taken from each individual skin sample to create a combined 600 µl skin secretion solution for each species. Ethanol was evaporated using a low-pressure nitrogen flow in a Rotavapor R-300 vacuum system (100 mbar, 35 °C). The resulting solute was then resuspended in 30 µl of ultrapure water containing 5% DMSO to facilitate the dilution of hydrophobic compounds.

Another five toxins found in dendrobatid frogs were shared by the Fitch lab (coauthor) from the John W. Daly laboratory collection (Daly 1995). Decahydroquinoline **195A** (DHQ **195A**, aka PTX-C, PTX-C_I), Synthetic racemic DHQ **167** HCl, (aka PTX-C_{IV}) was a generous gift of Dr. Larry Overman (Overman and Jessup 1978). Synthetic (+)-PTX **251D** HCl was prepared as described (Daly et al. 2003). Racemic octahydrohistrionicotoxin HCl (H8-HTX, HTX **291A**) was a generous gift of Dr. Yoshito Kishi (Fukuyama et al. 1975). Natural Histrionicotoxin (HTX **283A**) was isolated from mixed frog collections (Daly et al. 1971). were diluted in ultrapure water or ultrapure water plus 5% DMSO to obtain a 30nM to 100 nM stock dilution (Table S3).

Liver toxin neutralization assay

Generating liver soluble protein extracts

E. reginae ($n = 2$) and *C. tenuis* ($n = 1$) specimens were collected and euthanized according to approved UCB IACUC protocols (AUP-2019-08-12457) and a California Department of Fish and Wildlife Scientific Collecting Permit S-190980001-19111-001 (Table S1). Animals were humanely euthanized via decapitation, and liver samples were immediately dissected, flash-frozen, and stored at -80°C. Control mouse liver samples were collected from 5–6-week-old female CD1-IGS mice (Charles River Laboratories, Wilmington, MA, USA) under UCSF IACUC protocol AN076215-01F, and immediately flash-frozen in liquid nitrogen and stored at -80°C. Liver homogenization was adapted from descriptions of isolating soluble toxin-binding proteins from animal tissues by Llewellyn *et al.* 1997 and 1998. In brief, livers were

homogenized at approximately 1 ml per g of tissue in a buffer consisting of 10 mM Tris-HCl, 0.2 mM ethylenediaminetetraacetic acid (EDTA), pH 7.4, supplemented with EDTA-free protease inhibitor tablets (ThermoFisher Scientific, Waltham, MA, USA, Cat. A32955). Livers were homogenized using a PowerLyzer™ 24 bead beater with two cycles of 3500 rpm for 45 seconds, 30 seconds rest, and 3500 rpm for 45 seconds. Liver extracts were then centrifuged at 10,000 g for 15 minutes and the resultant pellet was discarded. The supernatant was filtered and then flash-frozen and stored at -80°C until use. Total protein was measured using the Pierce bicinchoninic acid (BCA) protein assay (ThermoFisher Scientific, cat. no. 23225) and extracts standardized to 0.2 mg/mL final concentration.

Mammalian cell culture

Chinese hamster ovary (CHO) cells stably expressing the α -subunit of the human skeletal muscle sodium channel isoform (*HsNa_v1.4*, NM_00334.4, B'SYS GmbH, cat. no. BSYS-Nav1.4-CHO-C) were maintained at 37°C, 5% CO₂ in culture medium containing Ham's F-12 medium with GlutaMAX (Gibco, cat. no. 31765035) supplemented with 9% (v/v) heat-inactivated fetal bovine serum (Gibco, cat. no. 16140071), penicillin-streptomycin (0.9% (v/v), Gibco, cat. no. 15-140-122) and 100 µg/mL Hygromycin B (Sigma-Aldrich, cat. no. 10843555001).

Whole-cell patch-clamp electrophysiology

The effects of treating toxins with liver extract on *HsNa_v1.4* were assessed using a semi-automated QPatch Compact II electrophysiology platform (Sophion Bioscience, Ballerup, Denmark). Recordings were conducted at 22°C. The intracellular solution (IC) contained the following in mM: 140 CsF, 1/5 EGTA/CsOH, 10 HEPES, 10 NaCl (pH 7.3 with 3M CsOH), 320 mOsm. The extracellular solution (EC, saline) contained the following in mM: 2 CaCl₂, 1 MgCl₂, 4 KCl, 145 NaCl, 10 HEPES, 10 glucose (pH 7.4 with NaOH), 305 mOsm. Solutions were filtered using a 0.22 µm membrane filter.

Before recording, cells were washed with Dulbecco's phosphate buffered saline (DPBS, Gibco, cat. no. 14190144), detached from culture flasks with Detachin (AMSBIO, cat. no. T100100) and then kept in serum-free medium (Sigma-Aldrich, cat. no. C5467) supplemented with 25 mM HEPES and 0.04 mg/mL soybean trypsin inhibitor (Sigma-Aldrich, cat. no. 10109886001). Immediately prior to recording, cells were washed and resuspended in EC to a final cell density of 4–6 x 10 cells/mL, and then applied to the QPatch Compact II (Sophion Bioscience, Ballerup, Denmark) using 8-channel QPlate 8X multihole chips (Sophion Bioscience, cat. no. SB0210).

Sodium currents were acquired at 25 kHz and filtered at 8333 kHz, with leak subtraction protocol applied and non-leak subtracted currents acquired in parallel. Sodium currents were elicited using a single pulse protocol where cells were held at -90 mV, with a hyperpolarization step of -120 mV for 200 ms followed by a depolarization step to 0 mV for 60 ms and then returned to a holding potential of -90 mV, with sweep-to-sweep interval duration of 10 seconds. All recordings were conducted at 22°C.

The effect of guanidinium toxins alone on *HsNa_v1.4* in CHO cells were first assessed by determining cumulative toxin concentration-response curves, with toxin solutions prepared in 3-fold serial dilution series in EC and applied as increasing concentrations. The IC₅₀ concentrations were calculated by fitting the concentration-response curves with non-linear

regression models in GraphPad Prism V10.0. Toxin concentrations sufficient to block ~90% of *HsNa_v1.4* currents were subsequently calculated using the IC_{50} and hillslope (H) as follows:

$$IC_x = \left(\frac{x}{100-x}\right)^{\frac{1}{H}} \times IC_{50}.$$

The effect of incubating toxin in liver extract was assessed by diluting samples in EC containing 0.05% w/v bovine serum albumin (BSA) and then incubating at room temperature ($23 \pm 2^\circ\text{C}$) for 30 min. Samples included: toxin alone; toxin combined with liver extract (0.2 mg/mL final); and liver extract alone (0.2 mg/mL). Where possible, toxin concentrations were selected with the aim of inhibiting 90% of sodium currents, which were calculated from the toxin concentration-response curves to be approximately 1.5 nM for neoSTX, 100 nM for STX, and 300 nM for TTX. In the case of frog-derived alkaloids, where toxin quantities were exceedingly limited, a single high concentration able to block putatively resistant *Erythrolamprus reginae* *ErNa_v1.4* by at least 60% was selected: 250 μM H₈-HTX; 500 μM HTX283A; 500 μM PTX251D; and *A. trivittata* skin extract (1:200 dilution). After incubating, these samples were applied to *HsNa_v1.4* cells, in stable whole-cell patch-clamp configuration with minimum of 1 nA of sodium current, in a successive fashion. First, steady baseline sodium currents were established in EC, followed by inhibiting currents with toxin-alone. Toxin samples were then washed out until currents returned to baseline, using at least nine chamber volumes of EC. The toxin:liver extract mix was then applied and compared against currents elicited in EC and toxin alone solutions. Finally, the toxin:liver extract mix was washed out and then liver extract alone was applied as a control. See Supplementary SF.3 for schematic of assay. All liver extracts and toxins were screened at minimum in duplicate in two independent assays. Normalized current recovery was then determined using the following equation: $\frac{I_{\text{toxin:liver}} - I_{\text{toxin}}}{I_{\text{control}} - I_{\text{toxin}}}$, where I_{control} is the baseline current elicited in EC, I_{toxin} is the current after application of toxin alone, and $I_{\text{toxin:liver}}$ is the current following application of the mixed toxin:liver extract. The degree of current recovery for each toxin between different species of liver extract was compared by one-way ANOVA with Tukey's post hoc test. All data analyses were performed using Sophion Analyzer software (Sophion Bioscience) and GraphPad Prism v10.0 (GraphPad Prism, San Diego, CA, USA).

Gene Reconstruction and Cloning of *E. reginae* Na_v1.4 (NR & R) and *HsNa_v1.4*

We used the *E. reginae* complete Na_v1.4 gene reconstruction from sample No. GECOH 2823 collected in Santa María, Boyacá, Colombia, with complete information published in Ramírez-Castañeda et al. (2024), as the template. Minor gaps in the sequence were completed using transcriptome samples generated in this study, employing BLAST v2.7.1+ to identify the required sites (Altschul et al. 1990).

Gene synthesis and cloning into the pcDNA3.1+ vector were requested from GenScript USA Inc. for two sequences: a non-resistant variant and a resistant variant of the *E. reginae* Na_v1.4 channel, following the sequences published in Ramírez-Castañeda et al. (2024) (*ErNa_v1.4* (NR) and *ErNa_v1.4* (R)) (see Fig. S1 & complete sequences in Dataset S4). Additionally, we ordered the complete synthesis and cloning of the human Na_v1.4 channel into pcDNA3.1 from the same company (Ref=CCDS:CCDS45761.1, protein_id=NP_000325.4) (*HsNa_v1.4*; GenScript USA Inc.) (complete sequences in Dataset S4).

In initial trials, the *ErNa_v1.4* (NR) and *ErNa_v1.4* (R) constructs were found to be unstable during replication. To address this, we used CopyCutter™ EPI400 Chemically Competent *E. coli* cells from VWR International and followed the recommended protocol.

Two-electrode voltage-clamp electrophysiology (TEVC)

Two-electrode voltage-clamp (TEVC) recordings were conducted using defolliculated *Xenopus laevis* oocytes at developmental stages V–VI. Oocytes were harvested following UCSF IACUC protocol AN178461, with recordings performed 1–2 days after microinjection with *HsNa_v1.4* mRNA and 3–4 days post-injection for *E. reginae* Na_v1.4 (NR & R). Linearized cDNA constructs were transcribed into capped mRNA using the mMACHINE T7 Transcription Kit (Invitrogen). Microinjections were performed using 9–16 ng of *HsNa_v1.4* mRNA and 50–64 ng of *E. reginae* Na_v1.4 (NR & R) mRNA. Data acquisition was carried out using a GeneClamp 500B amplifier (MDS Analytical Technologies) controlled by pClamp software (Molecular Devices), with signals digitized at 1 kHz using a Digidata 1332A digitizer (MDS Analytical Technologies). Oocytes were impaled with borosilicate glass microelectrodes (0.3–3.0 MΩ resistance) filled with 3 M KCl. Sodium currents were recorded in a bath solution (RS) composed of 96 mM NaCl, 1 mM CaCl₂, 1 mM MgCl₂, 2 mM KCl, and 5 mM HEPES (pH 7.5, adjusted with NaOH).

To determine the concentration–response relationship for STX, TTX, and neoSTX, test solutions containing specific toxin concentrations were sequentially applied via perfusion to oocytes expressing the channels ($n = 6$ oocytes, per Na_v channel and toxin). Sodium currents were elicited using a single-pulse protocol where oocytes were held at -120 mV for 3 s, followed by a depolarization step to 0 mV for 60 ms, before returning to -120 mV. The interval between sweeps was 10 s.

For STX and TTX, toxin block was washed out between concentrations (approximately 20 sweeps). For neoSTX, a cumulative toxin recording approach was used, where each concentration was maintained for ~50 sweeps. The IC₅₀ values (Fig. 2 and Table S4), representing the toxin concentration required to inhibit 50% of the current, were calculated by fitting concentration-response curves based on the ratio of peak currents in the presence and absence of toxin using the equation:

$$I_x = (I_{max} - I_{min}) / (1 + IC_x / IC_{50})$$

where I_x represents the current amplitude at toxin concentration x , I_0 is the current amplitude in the absence of toxin, and I_{max} and I_{min} correspond to the maximum and minimum peak current amplitudes, respectively.

Due to the limited availability of skin secretions and other dendrobatid toxins, a single toxin concentration was applied to the TEVC chamber for single-pulse recordings, followed by washout with buffer for ~50 sweeps ($n = 3$ oocytes per Na_v channel and toxin). The following toxin concentrations were used: a 1:100 dilution of *A. trivittata* and *S. ruber* skin extract, 500 μM H8-HTX, 500 μM HTX, 500 μM PTX251D, 1000 μM DHQ195A, and 1000 μM DHQ167. The available toxin quantities were insufficient to conduct tests with multiple concentrations. For statistical analysis, a non-parametric Mann-Whitney test was used to compare the reduction in current in the presence and absence of the toxin.

Activation and inactivation properties of each expressed Na_v channel were determined using specific voltage protocols. Inactivation was measured by holding the membrane potential at -120 mV for 30 ms, followed by incremental 10 mV depolarization steps for 600 ms, ending with a final step to 0 mV for 30 ms before returning to -120 mV. Activation was assessed by first applying a hyperpolarization step to -100 mV for 6.5 ms, followed by a depolarization from -100 mV to 70 mV by incremental 5 mV depolarization steps for 60 ms before returning to -120 mV.

References

- Abderemane-Ali F, Rossen ND, Kobiela ME, Craig RA, Garrison CE, Chen Z, Colleran CM, O'Connell LA, Bois JD, Dumbacher JP, et al. 2021. Evidence that toxin resistance in poison birds and frogs is not rooted in sodium channel mutations and may rely on “toxin sponge” proteins. *J. Gen. Physiol.* [Internet] 153. Available from: <https://doi.org/10.1085/jgp.202112872>
- Albarelli LPP, Santos-Costa MC. 2010. Feeding ecology of *Liophis reginae semilineatus* (Serpentes: Colubridae: Xenodontinae) in eastern Amazon, Brazil. *Zool. Curitiba* [Internet] 27:87–91. Available from: <http://www.scielo.br/j/zool/a/JzrKsdmm53NMWPDFf4wJz7L/?lang=en>
- Alexa A, Rahnenfuhrer J. 2022. topGO: Enrichment Analysis for Gene Ontology.
- Alonso E, Alfonso A, Vieytes MR, Botana LM. 2016. Evaluation of toxicity equivalent factors of paralytic shellfish poisoning toxins in seven human sodium channels types by an automated high throughput electrophysiology system. *Arch. Toxicol.* 90:479–488.
- Altschul SF, Gish W, Miller W, Myers EW, Lipman DJ. 1990. Basic local alignment search tool. *J. Mol. Biol.* 215:403–410.
- Alvarez-Buylla A, Fischer M-T, Moya Garzon MD, Rangel AE, Tapia EE, Tanzo JT, Soh HT, Coloma LA, Long JZ, O'Connell LA. 2023. Binding and sequestration of poison frog alkaloids by a plasma globulin. Radhakrishnan A, Schuman MC, editors. *eLife* [Internet] 12:e85096. Available from: <https://doi.org/10.7554/eLife.85096>
- Andresen BM, Bois JD. 2009. De novo Synthesis of Modified Saxitoxins for Sodium Ion Channel Study. *J. Am. Chem. Soc.* [Internet] 131:12524–12525. Available from: <https://www.ncbi.nlm.nih.gov/pmc/articles/PMC2770901/>
- Aubier TG, Sherratt TN. 2020. State-Dependent Decision-Making by Predators and Its Consequences for Mimicry. *Am. Nat.* [Internet] 196:E127–E144. Available from: <https://www.journals.uchicago.edu/doi/10.1086/710568>
- Barabas K, Faulk WP. 1993. Transferrin receptors associate with drug resistance in cancer cells. *Biochem. Biophys. Res. Commun.* 197:702–708.
- Candels LS, Becker S, Trautwein C. 2022. PLA2G7: a new player in shaping energy metabolism and lifespan. *Signal Transduct. Target. Ther.* [Internet] 7:1–2. Available from: <https://www.nature.com/articles/s41392-022-01052-5>
- Carle T, Rowe C. 2014. Avian predators change their foraging strategy on defended prey when undefended prey are hard to find. *Anim. Behav.* 93:97–103.
- Carlo RE del, Reimche JS, Moniz HA, Hague MTJ, Agarwal SR, Iii EDB, Jr EDB, Leblanc N, Feldman CR. 2024. Coevolution with toxic prey produces functional trade-offs in sodium channels of predatory snakes. *eLife* [Internet] 13. Available from: <https://elifesciences.org/reviewed-preprints/94633>

- Catterall WA. 2014. Structure and function of voltage-gated sodium channels at atomic resolution. *Exp. Physiol.* 99:35–51.
- Cei JM, Erspamer V, Roseghini M. 1967. Taxonomic and Evolutionary Significance of Biogenic Amines and Polypeptides Occurring in Amphibian Skin. I. Neotropical Leptodactylid Frogs. *Syst. Biol.* [Internet] 16:328–342. Available from: <https://doi.org/10.2307/2412152>
- Chen S. 2023. Ultrafast one-pass FASTQ data preprocessing, quality control, and deduplication using fastp. *iMeta* [Internet] 2:e107. Available from: <https://onlinelibrary.wiley.com/doi/abs/10.1002/imt2.107>
- Chen S, Zhou Y, Chen Y, Gu J. 2018. fastp: an ultra-fast all-in-one FASTQ preprocessor. *Bioinformatics* [Internet] 34:i884–i890. Available from: <https://doi.org/10.1093/bioinformatics/bty560>
- Chen Z, Zakrzewska S, Hajare HS, Alvarez-Buylla A, Abderemane-Ali F, Bogan M, Ramirez D, O'Connell LA, Du Bois J, Minor DL. 2022. Definition of a saxitoxin (STX) binding code enables discovery and characterization of the anuran saxiphilin family. *Proc. Natl. Acad. Sci.* [Internet] 119:e2210114119. Available from: <https://www.pnas.org/doi/10.1073/pnas.2210114119>
- Daly JW. 1995. The chemistry of poisons in amphibian skin. *Proc. Natl. Acad. Sci. U. S. A.* [Internet] 92:9–13. Available from: <http://www.ncbi.nlm.nih.gov/pubmed/7816854>
<http://www.pubmedcentral.nih.gov/articlerender.fcgi?artid=PMC42808>
- Daly JW. 1998. Thirty Years of Discovering Arthropod Alkaloids in Amphibian Skin †. 3864:162–172.
- Daly JW, Garraffo HM, Spande TF, Clark VC, Ma J, Ziffer H, Cover JF. 2003. Evidence for an enantioselective pumiliotoxin 7-hydroxylase in dendrobatid poison frogs of the genus *Dendrobates*. *Proc. Natl. Acad. Sci.* [Internet] 100:11092–11097. Available from: <https://www.pnas.org/doi/10.1073/pnas.1834430100>
- Daly JW, Karle I, Myers CW, Tokuyama T, Waters JA, Witkop B. 1971. Histrionicotoxins: Roentgen-Ray Analysis of the Novel Allenic and Acetylenic Spiroalkaloids Isolated from a Colombian Frog, *Dendrobates histrionicus*. *Proc. Natl. Acad. Sci.* [Internet] 68:1870–1875. Available from: <https://www.pnas.org/doi/10.1073/pnas.68.8.1870>
- Daly JW, Myers CW, Whittaker N. 1987. Further classification of skin alkaloids from neotropical poison frogs (Dendrobatidae), with a general survey of toxic/noxious substances in the amphibia. *Toxicon* [Internet] 25:1023–1095. Available from: <http://linkinghub.elsevier.com/retrieve/pii/0041010187902650>
- Damiani MT, Pavarotti M, Leiva N, Lindsay AJ, McCaffrey MW, Colombo MI. 2004. Rab Coupling Protein Associates with Phagosomes and Regulates Recycling from the Phagosomal Compartment. *Traffic* [Internet] 5:785–797. Available from: <https://onlinelibrary.wiley.com/doi/abs/10.1111/j.1600-0854.2004.00220.x>
- Darst CR, Cummings ME. 2006. Predator learning favours mimicry of a less-toxic model in poison frogs. *Nature* 440:208–211.

- Enge A-M, Kaltner F, Gottschalk C, Braeuning A, Hessel-Pras S. 2021. Active Transport of Hepatotoxic Pyrrolizidine Alkaloids in HepaRG Cells. *Int. J. Mol. Sci.* [Internet] 22:3821. Available from: <https://www.ncbi.nlm.nih.gov/pmc/articles/PMC8067754/>
- Engström K, Ameer S, Bernaudat L, Drasch G, Baeuml J, Skerfving S, Bose-O'Reilly S, Broberg K. 2013. Polymorphisms in genes encoding potential mercury transporters and urine mercury concentrations in populations exposed to mercury vapor from gold mining. *Environ. Health Perspect.* 121:85–91.
- Feder ME, Hofmann GE. 1999. HEAT-SHOCK PROTEINS, MOLECULAR CHAPERONES, AND THE STRESS RESPONSE: Evolutionary and Ecological Physiology. *Annu. Rev. Physiol.* [Internet] 61:243–282. Available from: <http://www.ncbi.nlm.nih.gov/pubmed/10099689>
<http://www.annualreviews.org/doi/10.1146/annurev.physiol.61.1.243>
- Feldman CR, Brodie ED, Brodie ED, Pfrender ME. 2012. Constraint shapes convergence in tetrodotoxin-resistant sodium channels of snakes. *Proc. Natl. Acad. Sci. U. S. A.* [Internet] 109:4556–4561. Available from: www.pnas.org/cgi/doi/10.1073/pnas.1113468109
- Feldman CR, Durso AM, Hanifin CT, Pfrender ME, Ducey PK, Stokes AN, Barnett KE, Brodie ED, Brodie ED. 2016. Is there more than one way to skin a newt? Convergent toxin resistance in snakes is not due to a common genetic mechanism. *Heredity* 116:84–91.
- Ferrer RP, Zimmer RK. 2012. Community Ecology and the Evolution of Molecules of Keystone Significance. *Biol. Bull.* [Internet] 223:167–177. Available from: <https://www.journals.uchicago.edu/doi/10.1086/BBLv223n2p167>
- Ferrer RP, Zimmer RK. 2013. Molecules of Keystone Significance: Crucial Agents in Ecology and Resource Management. *BioScience* [Internet] 63:428–438. Available from: <https://doi.org/10.1525/bio.2013.63.6.5>
- Fukuyama T, Dunkerton LV, Aratani M, Kishi Y. 1975. Synthetic studies on histrionicotoxins. II. Practical synthetic route to (+)-perhydro- and (+)-octahydrohistrionicotoxin. *J. Org. Chem.* [Internet] 40:2011–2012. Available from: <https://doi.org/10.1021/jo00901a038>
- Geffeney SL, Fujimoto E, Brodie ED, Brodie ED, Ruben PC. 2005. Evolutionary diversification of TTX-resistant sodium channels in a predator-prey interaction. *Nature* [Internet] 434:759–763. Available from: www.nature.com/nature.
- Halpin CG, Penacchio O, Lovell PG, Cuthill IC, Harris JM, Skelhorn J, Rowe C. 2020. Pattern contrast influences wariness in naïve predators towards aposematic patterns. *Sci. Rep.* [Internet] 10:9246. Available from: <https://www.nature.com/articles/s41598-020-65754-y>
- Halpin CG, Skelhorn J, Rowe C. 2013. Predators' decisions to eat defended prey depend on the size of undefended prey. *Anim. Behav.* [Internet] 85:1315–1321. Available from: <https://www.sciencedirect.com/science/article/pii/S0003347213001425>
- Halpin CG, Skelhorn J, Rowe C. 2014. Increased predation of nutrient-enriched aposematic prey. *Proc. R. Soc. B Biol. Sci.* [Internet] 281. Available from: <https://pubmed.ncbi.nlm.nih.gov/24598424/>

- Han Y-F, Fan X-H, Wang X-J, Sun K, Xue H, Li W-J, Wang Y-B, Chen J-Z, Zhen Y-S, Zhang W-L, et al. 2011. Association of intergenic polymorphism of organic anion transporter 1 and 3 genes with hypertension and blood pressure response to hydrochlorothiazide. *Am. J. Hypertens.* 24:340–346.
- Hurlbert SH. 1970. Predator Responses to the Vermilion-Spotted Newt (*Notophthalmus viridescens*). *J. Herpetol.* [Internet] 4:47–55. Available from: <https://www.jstor.org/stable/1562702>
- Jeckel AM, Kocheff S, Saporito RA, Grant T. 2019. Geographically separated orange and blue populations of the Amazonian poison frog *Adelphobates galactonotus* (Anura, Dendrobatidae) do not differ in alkaloid composition or palatability. *Chemoecology* [Internet] 29:225–234. Available from: <https://link.springer.com/article/10.1007/s00049-019-00291-3>
- Jeckel AM, Saporito RA, Grant T. 2015. The relationship between poison frog chemical defenses and age, body size, and sex. *Front. Zool.* [Internet] 12:27. Available from: <https://doi.org/10.1186/s12983-015-0120-2>
- Jia L, Betters JL, Yu L. 2011. Niemann-Pick C1-Like 1 (NPC1L1) Protein in Intestinal and Hepatic Cholesterol Transport. *Annu. Rev. Physiol.* [Internet] 73:239–259. Available from: <https://www.ncbi.nlm.nih.gov/pmc/articles/PMC3965667/>
- Kawai K, Negoro R, Ichikawa M, Yamashita T, Deguchi S, Harada K, Hirata K, Takayama K, Mizuguchi H. 2020. Establishment of SLC15A1/PEPT1-Knockout Human-Induced Pluripotent Stem Cell Line for Intestinal Drug Absorption Studies. *Mol. Ther. Methods Clin. Dev.* [Internet] 17:49–57. Available from: [https://www.cell.com/molecular-therapy-family/methods/abstract/S2329-0501\(19\)30133-0](https://www.cell.com/molecular-therapy-family/methods/abstract/S2329-0501(19)30133-0)
- Kemp MI, Kemp AC. 1978. Bucorvus and Sagittarius: Two Modes of Terrestrial Predation. In: Proceedings of the Symposium on African Predatory Birds. Pretoria: Northern Transvaal Ornithological Society.
- Kim D, Langmead B, Salzberg SL. 2015. HISAT: a fast spliced aligner with low memory requirements. *Nat. Methods* [Internet] 12:357–360. Available from: <https://www.nature.com/articles/nmeth.3317>
- Lawrence JP, Rojas B, Fouquet A, Mappes J, Blanchette A, Saporito RA, Bosque RJ, Courtois EA, Noonan BP. 2019. Weak warning signals can persist in the absence of gene flow. *Proc. Natl. Acad. Sci.* [Internet] 116:19037–19045. Available from: <https://www.pnas.org/doi/full/10.1073/pnas.1901872116>
- Le TNU, Nguyen TQ, Kalailingam P, Nguyen YTK, Sukumar VK, Tan CKH, Tukijan F, Couty L, Hasan Z, Del Gaudio I, et al. 2022. *Mfsd2b* and *Spns2* are essential for maintenance of blood vessels during development and in anaphylactic shock. *Cell Rep.* [Internet] 40:111208. Available from: <https://www.sciencedirect.com/science/article/pii/S2211124722010257>
- Li Y, Jiang Y, Zhang Y, Li N, Yin Q, Liu L, Lv X, Liu Yan, Li A, Fang B, et al. 2021. Abnormal upregulation of cardiovascular disease biomarker PLA2G7 induced by proinflammatory

- macrophages in COVID-19 patients. *Sci. Rep.* [Internet] 11:6811. Available from: <https://www.nature.com/articles/s41598-021-85848-5>
- Llewellyn LE, Bell PM, Moczydlowski EG. 1997. Phylogenetic survey of soluble saxitoxin-binding activity in pursuit of the function and molecular evolution of saxiphilin, a relative of transferrin. *Proc. Biol. Sci.* 264:891–902.
- Love MI, Huber W, Anders S. 2014. Moderated estimation of fold change and dispersion for RNA-seq data with DESeq2. *Genome Biol.* 15:550.
- Mahar J, Lukács GL, Li Y, Hall S, Moczydlowski E. 1991. Pharmacological and biochemical properties of saxiphilin, a soluble saxitoxin-binding protein from the bullfrog (*Rana catesbeiana*). *Toxicol. Off. J. Int. Soc. Toxicology* 29:53–71.
- Mappes J, Kokko H, Ojala K, Lindström L. 2014. Seasonal changes in predator community switch the direction of selection for prey defences. *Nat. Commun.* [Internet] 5:5016. Available from: <https://www.nature.com/articles/ncomms6016>
- María Arenas L, Walter D, Stevens M. 2015. Signal honesty and predation risk among a closely related group of aposematic species. *Sci. Rep.* [Internet] 5:11021. Available from: <https://www.nature.com/articles/srep11021>
- Márquez R, Ramírez-Castañeda V, Amézquita A. 2019. Does batrachotoxin autoresistance coevolve with toxicity in Phyllobates poison-dart frogs? *Evolution* [Internet] 73:390–400. Available from: <https://onlinelibrary.wiley.com/doi/abs/10.1111/evo.13672>
- Marshall GAK. 1908. On Diaposematism, with reference to some limitations of the Müllerian Hypothesis of Mimicry. *Trans. R. Entomol. Soc. Lond.* [Internet] 56:93–142. Available from: <https://onlinelibrary.wiley.com/doi/abs/10.1111/j.1365-2311.1908.tb02141.x>
- McGlothlin JW, Chuckalovcak JP, Janes DE, Edwards SV, Feldman CR, Brodie ED, Pfrender ME. 2014. Parallel evolution of tetrodotoxin resistance in three voltage-gated sodium channel genes in the garter snake *Thamnophis sirtalis*. *Mol. Biol. Evol.* 31:2836–2846.
- Mohammadi S, Gompert Z, Gonzalez J, Takeuchi H, Mori A, Savitzky AH. 2016. Toxin-resistant isoforms of Na⁺/K⁺-ATPase in snakes do not closely track dietary specialization on toads. *Proc. R. Soc. B Biol. Sci.* [Internet] 283:20162111. Available from: <https://royalsocietypublishing.org/doi/full/10.1098/rspb.2016.2111>
- Mohammadi S, Yang L, Harpak A, Herrera-Álvarez S, Rodríguez-Ordoñez M del P, Peng J, Zhang K, Storz JF, Dobler S, Crawford AJ, et al. 2021. Concerted evolution reveals co-adapted amino acid substitutions in Na⁺/K⁺-ATPase of frogs that prey on toxic toads. *Curr. Biol.* [Internet]. Available from: <https://linkinghub.elsevier.com/retrieve/pii/S0960982221004620>
- Morabito MA, Moczydlowski E. 1995. Molecular cloning of bullfrog saxiphilin: a unique relative of the transferrin family that binds saxitoxin. *Proc. Natl. Acad. Sci. U. S. A.* 92:6651.
- Nigam SK. 2015. What do drug transporters really do? *Nat. Rev. Drug Discov.* [Internet] 14:29–44. Available from: <https://www.ncbi.nlm.nih.gov/pmc/articles/PMC4750486/>

- Overman LE, Jessup PJ. 1978. Synthetic applications of N-acylamino-1,3-dienes. An efficient stereospecific total synthesis of dl-pumiliotoxin C, and a general entry to cis-decahydroquinoline alkaloids. *J. Am. Chem. Soc.* [Internet] 100:5179–5185. Available from: <https://doi.org/10.1021/ja00484a046>
- Pašukonis A, Loretto M-C. 2020. Predation on the Three-striped poison frog, *Ameerega trivitatta* (Boulenger 1884; Anura: Dendrobatidae), by *Erythrolamprus reginae* (Linnaeus 1758; Squamata: Collubridae). Available from: <https://www.biotaxa.org/hn/article/view/60062>
- Pearson KC, Tarvin RD. 2022. A review of chemical defense in harlequin toads (Bufonidae: Atelopus). *Toxicon X* [Internet] 13:100092. Available from: <https://www.sciencedirect.com/science/article/pii/S2590171022000029>
- Peelman F, Labeur C, Vanloo B, Roosbeek S, Devaud C, Duverger N, Denèfle P, Rosier M, Vandekerckhove J, Rosseneu M. 2003. Characterization of the ABCA transporter subfamily: identification of prokaryotic and eukaryotic members, phylogeny and topology. *J. Mol. Biol.* 325:259–274.
- Pertea G, Pertea M. 2020. GFF Utilities: GffRead and GffCompare. Available from: <https://f1000research.com/articles/9-304>
- Pizzagalli MD, Bensimon A, Superti-Furga G. 2021. A guide to plasma membrane solute carrier proteins. *FEBS J.* [Internet] 288:2784–2835. Available from: <https://onlinelibrary.wiley.com/doi/abs/10.1111/febs.15531>
- Prates I, Antoniazzi MM, Sciani JM, Pimenta DC, Toledo LF, Haddad CFB, Jared C. 2012. Skin glands, poison and mimicry in dendrobatid and leptodactylid amphibians. *J. Morphol.* 273:279–290.
- Putri GH, Anders S, Pyl PT, Pimanda JE, Zanini F. 2022. Analysing high-throughput sequencing data in Python with HTSeq 2.0. *Bioinformatics* [Internet] 38:2943–2945. Available from: <https://doi.org/10.1093/bioinformatics/btac166>
- Ramírez-Castañeda V, Tarvin R, Marquez R. 2024. Snakes (*Erythrolamprus* spp.) with a complex toxic diet show convergent yet highly heterogeneous voltage-gated sodium channel evolution. Available from: <https://ecoevorxiv.org/repository/view/7449/>
- Rowland HM, Fulford AJT, Ruxton GD. 2017. Predator learning differences affect the survival of chemically defended prey. *Anim. Behav.* [Internet] 124:65–74. Available from: <https://www.sciencedirect.com/science/article/pii/S0003347216303268>
- Ruiz-Mazón L, Ramírez-Rico G, Garza M de la. 2024. Lactoferrin: a secret weapon in the war against pathogenic bacteria. *Explor. Drug Sci.* [Internet] 2:734–743. Available from: <https://www.explorationpub.com/Journals/eds/Article/100872>
- Santos JC, Tarvin RD, O'Connell LA. 2016. A Review of Chemical Defense in Poison Frogs (Dendrobatidae): Ecology, Pharmacokinetics, and Autoresistance. In: Schulte BA, Goodwin TE, Ferkin MH, editors. *Chemical Signals in Vertebrates 13*. Cham: Springer International Publishing. p. 305–337.
- Saporito RA, Donnelly MA, Spande TF, Garraffo HM. 2011. A review of chemical ecology in

- poison frogs. *Chemoecology* [Internet] 22:159–168. Available from: <http://link.springer.com/10.1007/s00049-011-0088-0>
- Sherratt TN. 2003. State-dependent risk-taking by predators in systems with defended prey. *Oikos* [Internet] 103:93–100. Available from: <https://onlinelibrary.wiley.com/doi/abs/10.1034/j.1600-0706.2003.12576.x>
- Sherratt TN, Speed MP, Ruxton GD. 2004. Natural selection on unpalatable species imposed by state-dependent foraging behaviour. *J. Theor. Biol.* [Internet] 228:217–226. Available from: <https://www.sciencedirect.com/science/article/pii/S0022519304000049>
- Skelhorn J, Halpin CG, Rowe C. 2016. Learning about aposematic prey. *Behav. Ecol.* 27:955–964.
- Skelhorn J, Rowe C. 2007. Predators' Toxin Burdens Influence Their Strategic Decisions to Eat Toxic Prey. *Curr. Biol.* [Internet] 17:1479–1483. Available from: <https://www.sciencedirect.com/science/article/pii/S0960982207017885>
- Skelhorn J, Rowland HM, Delf J, Speed MP, Ruxton GD. 2011. Density-dependent predation influences the evolution and behavior of masquerading prey. *Proc. Natl. Acad. Sci.* [Internet] 108:6532–6536. Available from: <https://www.pnas.org/doi/10.1073/pnas.1014629108>
- Smith C, Cranfield J, Allain SJR. 2024. 'Stress and wash' may make great crested *Triturus cristatus* and smooth newts *Lissotriton vulgaris* palatable for grey herons *Ardea cinerea*, with a link to video evidence. *Herpetol. Bull.* [Internet]:33–34. Available from: <https://www.thebhs.org/publications/the-herpetological-bulletin/issue-number-170-winter-2024/4226-08-stress-and-wash-may-make-great-crested-i-triturus-cristatus-i-and-smooth-newts-lissotriton-vulgaris-palatable-for-grey-herons-i-ardea-cinerea-i-with-a-link-to-video-evidence>
- Speed MP. 1993. Muellerian mimicry and the psychology of predation. *Anim. Behav.* 45:571–580.
- Spolaore B, Fernández J, Lomonte B, Massimino ML, Tonello F. 2019. Enzymatic labelling of snake venom phospholipase A2 toxins. *Toxicon* [Internet] 170:99–107. Available from: <https://www.sciencedirect.com/science/article/pii/S0041010119304696>
- Tarvin RD, Borghese CM, Sachs W, Santos JC, Lu Y, O'Connell LA, Cannatella DC, Harris RA, Zakon HH. 2017. Interacting amino acid replacements allow poison frogs to evolve epibatidine resistance. *Science* 357:1261–1266.
- Tarvin RD, Pearson KC, Douglas TE, Ramírez-Castañeda V, Navarrete MJ. 2023. The Diverse Mechanisms that Animals Use to Resist Toxins. *Annu. Rev. Ecol. Evol. Syst.* [Internet] 54:null. Available from: <https://doi.org/10.1146/annurev-ecolsys-102320-102117>
- Terlau H, Heinemann SH, Stühmer W, Pusch M, Conti F, Imoto K, Numa S. 1991. Mapping the site of block by tetrodotoxin and saxitoxin of sodium channel II. *FEBS Lett.* [Internet] 293:93–96. Available from: <https://www.sciencedirect.com/science/article/pii/0014579391811596>

- van Thiel J, Khan MA, Wouters RM, Harris RJ, Casewell NR, Fry BG, Kini RM, Mackessy SP, Vonk FJ, Wüster W, et al. 2022. Convergent evolution of toxin resistance in animals. *Biol. Rev.* [Internet] 97:1823–1843. Available from: <https://onlinelibrary.wiley.com/doi/abs/10.1111/brv.12865>
- Tortorella S, Karagiannis TC. 2014. Transferrin Receptor-Mediated Endocytosis: A Useful Target for Cancer Therapy. *J. Membr. Biol.* [Internet] 247:291–307. Available from: <https://link.springer.com/article/10.1007/s00232-014-9637-0>
- Ujvari B, Casewell NR, Sunagar K, Arbuckle K, Wüster W, Lo N, O’Meally D, Beckmann C, King GF, Deplazes E, et al. 2015. Widespread convergence in toxin resistance by predictable molecular evolution. *Proc. Natl. Acad. Sci.* [Internet] 112:11911–11916. Available from: <https://www.pnas.org/doi/full/10.1073/pnas.1511706112>
- Underhill R. 2015. Mayne Island, B.C. Wetlands and Amphibian Habitats. Mayne Island Conservancy Society
- Vaelli PM, Theis KR, Williams JE, O’Connell LA, Foster JA, Eisthen HL. 2020. The skin microbiome facilitates adaptive tetrodotoxin production in poisonous newts. Baldwin IT, Robert CA, Robert CA, González Montoya MC, editors. *eLife* [Internet] 9:e53898. Available from: <https://doi.org/10.7554/eLife.53898>
- Vu TM, Ishizu A-N, Foo JC, Toh XR, Zhang F, Whee DM, Torta F, Cazenave-Gassiot A, Matsumura T, Kim S, et al. 2017. Mfsd2b is essential for the sphingosine-1-phosphate export in erythrocytes and platelets. *Nature* [Internet] 550:524–528. Available from: <https://www.nature.com/articles/nature24053>
- Waizenegger J, Glück J, Henricsson M, Luckert C, Braeuning A, Hessel-Pras S. 2021. Pyrrolizidine Alkaloids Disturb Bile Acid Homeostasis in the Human Hepatoma Cell Line HepaRG. *Foods* [Internet] 10:161. Available from: <https://www.ncbi.nlm.nih.gov/pmc/articles/PMC7828834/>
- Williams BL, Hanifin CT, Brodie ED, III EDB. 2010. Tetrodotoxin affects survival probability of rough-skinned newts (*Taricha granulosa*) faced with TTX-resistant garter snake predators (*Thamnophis sirtalis*). *Chemoecology* [Internet] 20:285–290. Available from: <http://link.springer.com/10.1007/s00049-010-0057-z>
- Yee SW, Nguyen AN, Brown C, Savic RM, Zhang Y, Castro RA, Cropp CD, Choi JH, Singh D, Tahara H, et al. 2013. Reduced renal clearance of cefotaxime in asians with a low-frequency polymorphism of OAT3 (SLC22A8). *J. Pharm. Sci.* 102:3451–3457.
- Yen T-J, Lolicato M, Thomas-Tran R, Du Bois J, Minor DL. 2019. Structure of the saxiphilin:saxitoxin (STX) complex reveals a convergent molecular recognition strategy for paralytic toxins. *Sci. Adv.* [Internet] 5:eaax2650. Available from: <https://www.science.org/doi/10.1126/sciadv.aax2650>
- Yotsu-Yamashita M, Sugimoto A, Terakawa T, Shoji Y, Miyazawa T, Yasumoto T. 2001. Purification, characterization, and cDNA cloning of a novel soluble saxitoxin and tetrodotoxin binding protein from plasma of the puffer fish, *Fugu pardalis*. *Eur. J. Biochem.* 268:5937–5946.

Zakrzewska S, Nixon SA, Chen Z, Hajare HS, Park ER, Mulcahy JV, Arlinghaus KM, Neu E, Konovalov K, Provasi D, et al. 2025. Structural basis for saxitoxin congener binding and neutralization by anuran saxiphilins. *Nat. Commun.* [Internet] 16:3885. Available from: <https://www.nature.com/articles/s41467-025-58903-2>

SUPPLEMENTARY INFORMATION

Supplementary figures

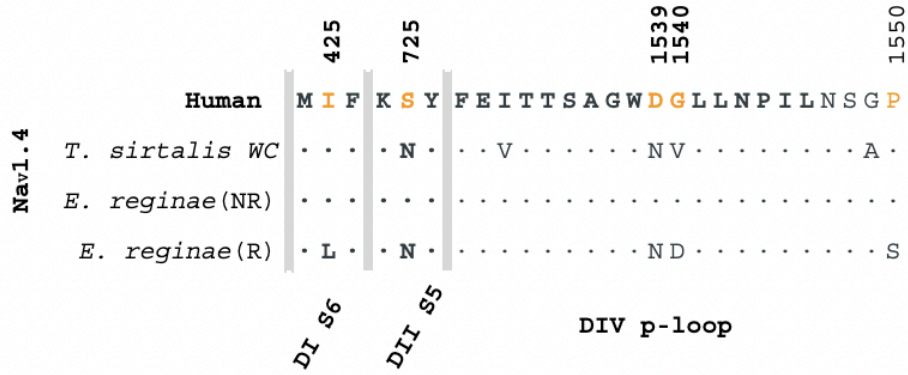


Figure S1. The set of amino acid differences between *E. reginae* non-resistant and resistant Nav1.4 variants introduced the cloning vector.

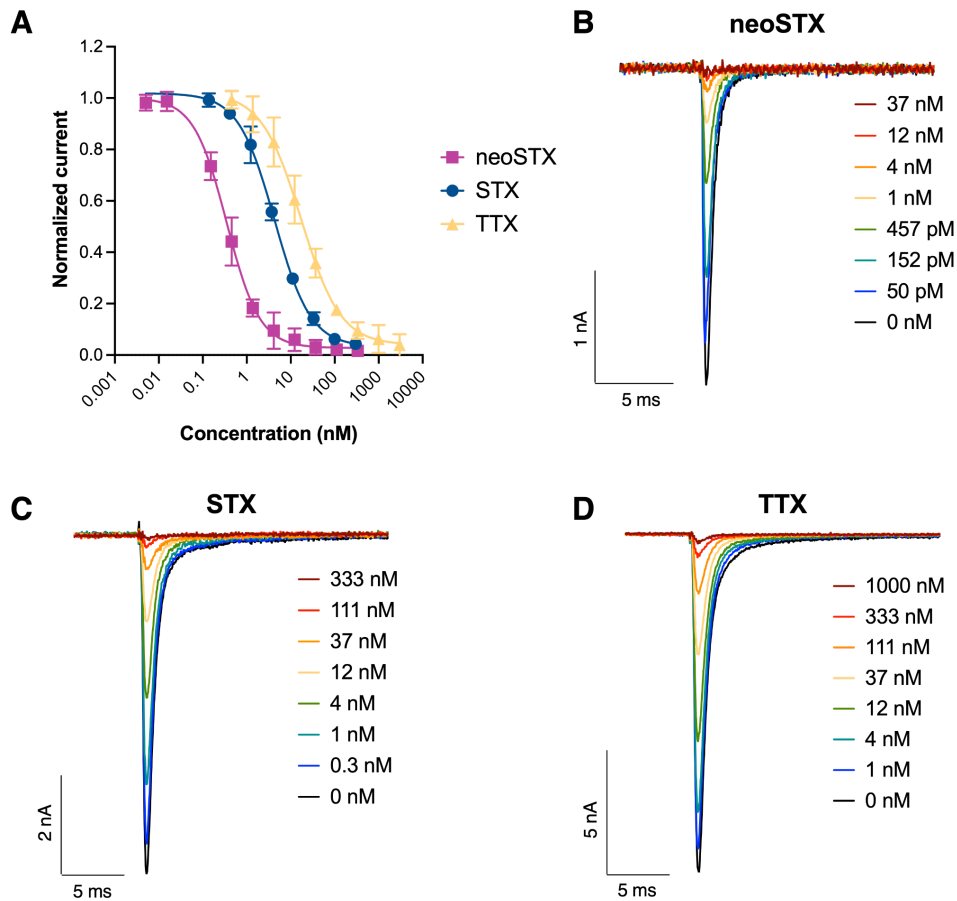


Figure S2. Whole-cell patch-clamp recordings of *HsNav*_{1.4} responses to guanidinium toxins. (A) Concentration-response curves to neoSTX (purple, squares), STX (blue, circles) and TTX (yellow, triangles). Each point represents the mean with standard deviation, $n = 5-6$ cells. (B-D) Exemplar whole-cell patch-clamp recordings for increasing concentrations of toxins for neoSTX (B), STX (C), and TTX (D).

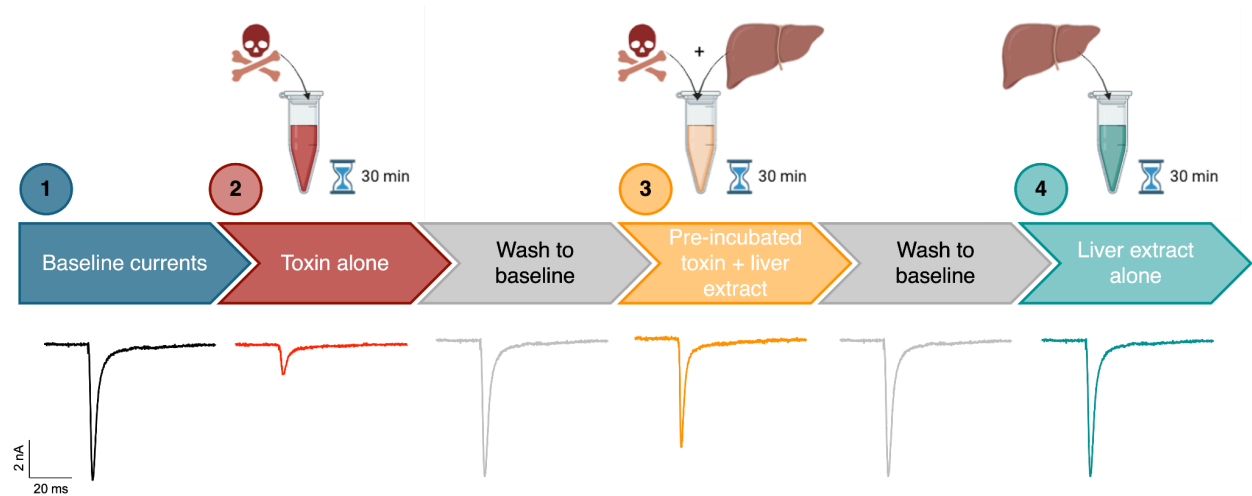


Fig S3. Schematic for liver extract functional toxin neutralization assay with example *HsNav*_{1.4} currents. The capacity for liver protein extracts from different organisms to inhibit the toxin block of *HsNav*_{1.4} were measured by planar patch-clamp assay using a QPatch Compact II (Sophion Bioscience). Cells were sequentially exposed to four different conditions, with wash steps between: **1. Baseline currents** in ECS (blue), with no toxin or liver extract. **2. Toxin alone** (red), TTX, STX, neoSTX, PTX251D, H8-HTX, HTX283A, and *A. trivittata* skin secretion were diluted in ECS to concentrations sufficient to inhibit *HsNav*_{1.4} currents by at least 60% and were pre-incubated for 30 minutes before addition to cells. **3. Toxin:liver extract mixture** (yellow), toxins from (2) were pre-incubated for 30 minutes at room temperature with liver extracts (final concentration 0.2 mg/mL) from *E. reginae*, *C. tenuis* (a control species of Colubrid snake from California, USA, with no known exposure to dendrobatid toxins), and mouse liver. If the toxin block observed in (2) was reduced in the presence of a liver extract, we inferred that the extract contained a detoxifying or toxin-binding protein. **4. Liver alone** (teal), liver extracts alone (final concentration 0.2 mg/mL) were incubated for 30 minutes at room temperature and added to the cells. If the liver extract alone affected sodium channel function, it would indicate intrinsic toxicity to *HsNav*_{1.4}. Figure was partially generated using <https://Biorender.com>.

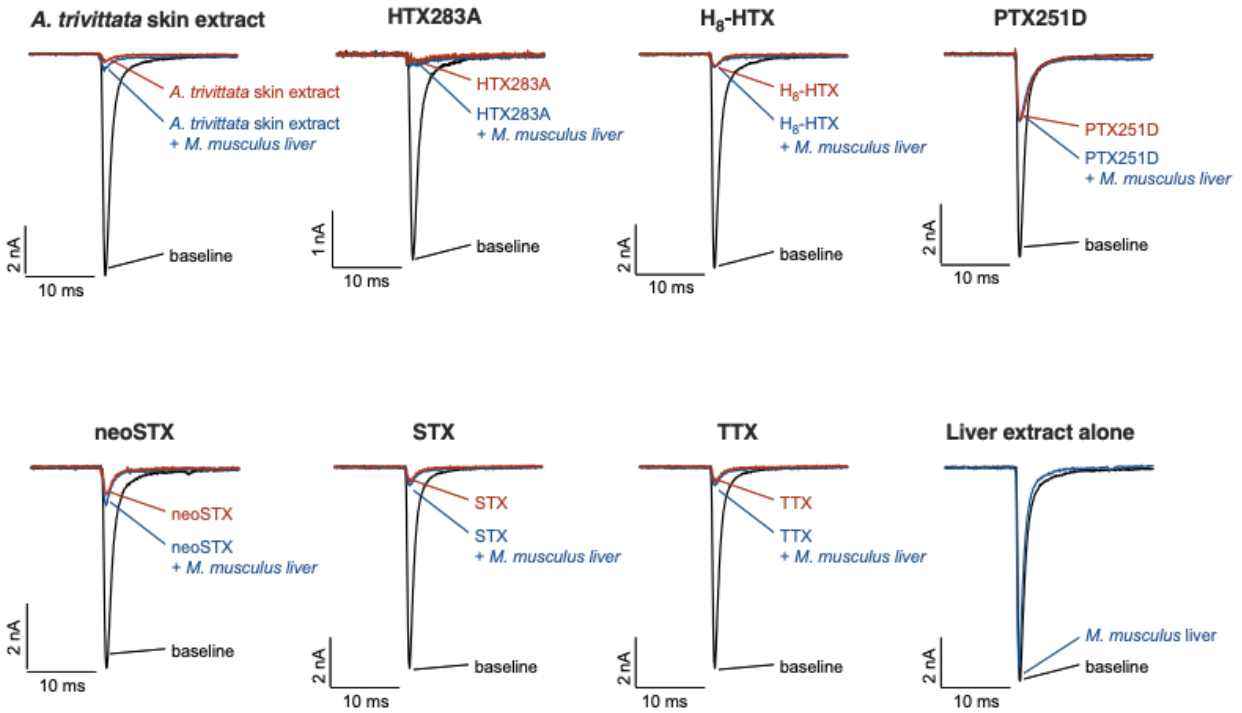


Figure S4. Mouse liver extract does not affect toxin block of $HsNa_v1.4$. Exemplar whole-cell patch-clamp recordings of $HsNa_v1.4$ expressed in CHO cells in the absence of toxin (baseline, black), presence of toxin alone (maroon) and toxin mixed with *M. musculus* liver extract (blue). Toxin concentrations used: *A. trivittata* skin extract diluted 1:200; HTX283A, 500 μ M; H₈-HTX, 250 μ M; PTX251D, 500 μ M; neoSTX, 1.5 nM; STX, 100 nM; TTX, 300 nM. Final liver concentration was 0.2 mg/mL.

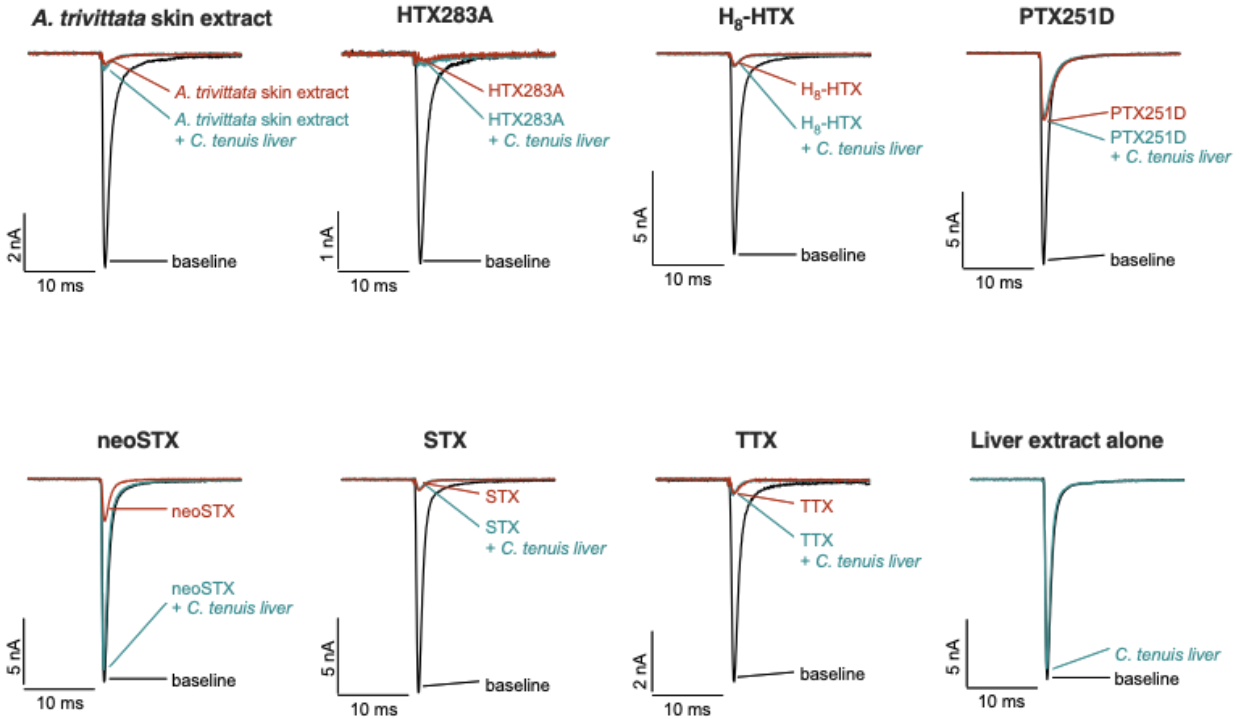


Figure S5. *C. tenuis* liver extract ameliorates neoSTX block of $HsNa_v1.4$, but does not affect STX, TTX or dendrobatid toxin block. Exemplar whole-cell patch-clamp recordings of $HsNa_v1.4$ expressed in CHO cells in the absence of toxin (baseline, black), presence of toxin alone (maroon), and toxin mixed with *C. tenuis* liver extract (teal). Toxin concentrations used: *A. trivittata* skin extract diluted 1:200; HTX283A, 500 μ M; H_8 -HTX, 250 μ M; PTX251D, 500 μ M; neoSTX, 1.5 nM; STX, 100 nM; TTX, 300 nM. Final liver concentration was 0.2 mg/mL.

Fig. S6. Transcriptomic responses of *E. reginae* after consumption of *A. trivittata*, *S. ruber*, or under fasting conditions. (A) Principal Component Analysis (PCA) of variance-stabilized transformed (VST) transcriptomic data from the DESeq2 package (REF) across four tissues (tongue, liver, stomach, and intestine) under three dietary conditions: consumption of *A. trivittata*, *S. ruber*, or fasting. The sample Er113_Li_S9 correspond to the snake that died after *A. trivittata* ingestion (see Table S2). (C) Volcano plots showing differentially expressed genes across all tissues and in liver tissue for two pairwise comparisons: fasting vs. *A. trivittata* and *S. ruber* vs. *A. trivittata*. Gene families previously associated with toxin resistance were highlighted, including solute carriers (SLC), phospholipases (PLA2), cytochrome P450s (CYP), serpins (SERPIN), ATP-binding cassette transporters (ABC), heat shock proteins (HSP), Rab GTPases (RAB), cholinesterase-like genes, transferrin-related genes, lactotransferases and other *E. reginae* genes annotated in NCBI as transporters. (D) Circular plot showing liver-specific Gene Ontology (GO) enrichment analysis for upregulated genes under the cellular component category, using topGO (REF). Each segment represents a GO term, with segment width corresponding to the number of upregulated genes annotated with that term (“Significant” value).

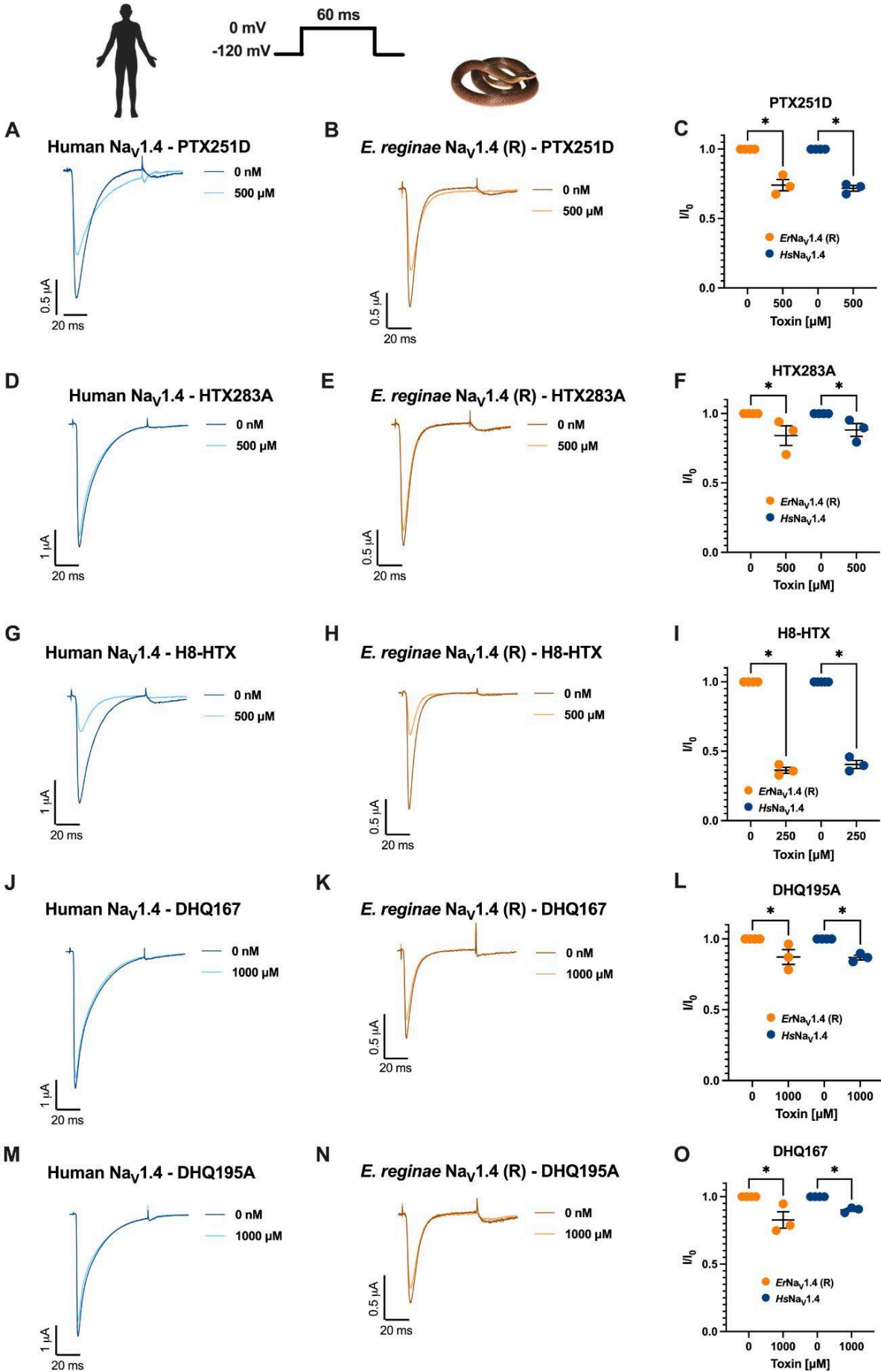


Figure S7. *E. reginae* Na_v1.4 resistant variant is sensitive to other toxins found in dendrobatid frogs (B, E, H, K, N). Exemplar current recordings for Human Na_v1.4 (*HsNa_v1.4* in blue), and *E. reginae* Na_v1.4 resistant variant (*ErNa_v1.4* (R) in orange) expressed in oocytes cells and exposed to (+)-pumiliotoxin 251D (PTX251D), histrionicotoxin 283A (HTX283A), (+/-)-H8-histrionicotoxin (H8-HTX), decahydroquinoline 167 (DHQ167), and decahydroquinoline 195A (DHQ195A). Comparison of sodium current reduction in the presence or absence of 500 μM PTX251D (C), 500 μM HTX283A (F), 500 μM H8-HTX (I), 1000 μM DHQ167 (L), and 1000 μM DHQ195A (O). Statistical significance was assessed using a Kruskal-Wallis test, with p-values provided for the corresponding comparisons. P-values are shown in the graph as (ns) P > 0.05; (*) P ≤ 0.05; (**) P ≤ 0.01; (***) P ≤ 0.001.

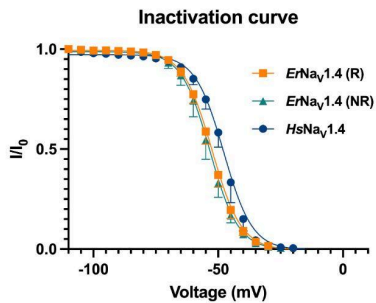


Figure S8. Inactivation and activation curve (to be updated) for the *E. reginae* Na_v1.4 “resistant” (R) and “non-resistant” (NR), and the human Na_v1.4.

Supplementary tables (See here:

https://docs.google.com/spreadsheets/d/1bSulrsMI8L7C_3hZPtOSqGRSR9JkD7ROVfBWVaMfnE0/edit?usp=sharing)

Table S1. General information and descriptions of the samples used in experimental assays, including museum specimen accession numbers and collection data.

Table S2. Samples used for transcriptome analysis, including RIN values, SRA accession numbers, experimental condition, and tissue type.

Table S3. Stock and dilution details for toxins PTX251D, HTX283A, H8-HTX, DHQ167, and DHQ195A.

Table S4. IC₅₀ values for TTX, STX, and neoSTX for *E. reginae* Na_v1.4 “resistant” (R) and “non-resistant” (NR) variants, and human Na_v1.4.

Table S5. Inactivation and activation V₅₀ and slope (K) values for *E. reginae* Na_v1.4 “resistant” (R) and “non-resistant” (NR) variants, and human Na_v1.4.

Table S6. List of genes annotated as transporters in the *E. reginae* NCBI genome annotation.

Supplementary datasets (See here:

<https://drive.google.com/drive/folders/17Sn28lbvKRmHFtlkuXo8rEIX5Jkc-pz?usp=sharing>)

Dataset S1. Recording of *E. reginae* feeding on *S. ruber*. Field sample number VRC19.

Dataset S2. Recording extract of dragging behavior of *E. reginae* feeding on *A. trivittata*. Field sample number VRC101.

Dataset S3. *E. reginae* NCBI annotation of upregulated genes across four tissues (tongue, liver, stomach, and intestine) under three dietary conditions: consumption of *A. trivittata*, *S. ruber*, or fasting.

Dataset S4. pcDNA3.1+ expression vectors containing the *E. reginae* Na_v1.4 “resistant” (R) and “non-resistant” (NR), and the human Na_v1.4 coding sequence.

Dataset S5. Domain IV sequences of the *E. reginae* Na_v1.4 channel from field samples VRC10 and VRC09, used in the liver extract screening assay for functional toxin neutralization.

Dataset S6. Complete results from the chemical analysis using gas chromatography mass spectrometry (GC/MS) of 6 *S. ruber* and 6 *A. trivittata* skins (to be uploaded).

Dataset S7. Complete manuscript in Spanish. The Spanish translation was produced using ChatGPT and edited by VRC (OpenAI, 2023) (to be uploaded).